WATER BASED SOL-GEL SYNTHESIS AND CHARACTERIZATION OF HYDROXYAPATITE

A DISSERTATION REPORT

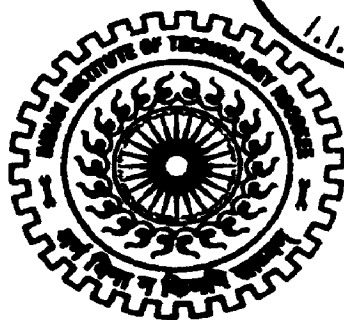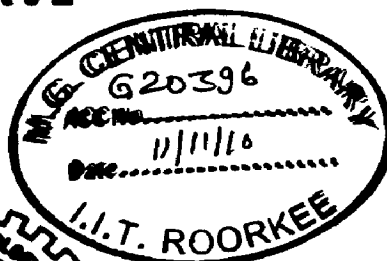*Submitted in partial fulfillment of the award of the degree*
of
MASTER OF TECHNOLOGY
in
NANOTECHNOLOGY

By

GYANAVI

CENTRE OF NANOTECHNOLOGY
INDIAN INSTITUTE OF TECHNOLOGY ROORKEE
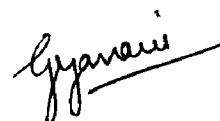ROORKEE - 247 667 (INDIA)
JUNE, 2010

CANDIDATE'S DECLARATION

*I hereby declare that the work, which is being presented in this dissertation entitled "WATER BASED SOL-GEL SYNTHESIS AND CHARACTERIZATION OF HYDROXYAPATITE" submitted in partial fulfillment of the requirement for the award of degree of **Master of Technology in NANOTECHNOLOGY**, submitted in the **Centre of Nanotechnology, Indian Institute of Technology Roorkee**, is an authentic record of my own work carried out under the guidance of **Dr. K. L. Yadav** , Associate Professor, Department of Physics and **Dr. G.D. Varma** , Associate Professor ,Department of Physics, Indian Institute of Technology Roorkee, Roorkee.*

The matter embodied in this dissertation work has not been submitted by me for the award of any other degree of this or any other Institute/ University. In keeping with the general practice of reporting scientific observation, due acknowledgement has been made wherever the work described is based on the finding of other investigators.
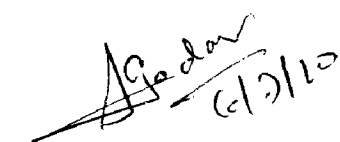
Date:

Place: Roorkee

(GYANAVI)

CERTIFICATE

This is to certify that the above declaration made by the candidate is correct to the best of our knowledge and belief.

Dr. G.D. Varma
Associatet Professor
Deptt. of Physics
IIT Roorkee

Dr. K.L. Yadav
Associate Professor
Deptt. of Physics
IIT Roorkee

ACKNOWLEDGEMENT

Firstly, I would like to thank my supervisors Dr. K.L. Yadav and Dr. G.D. Varma, Associate Professors, Department of Physics, I.I.T. Roorkee, for their valuable guidance, continuous support and discussions at various stages of the work. It is because of their inspiring presence, positive attitude, continuous encouragement, great care and tender treatment that this thesis could be brought to the present form within stipulated frame.

I also would like to extend my gratitude towards the PhD scholars of Physics Department, I.I.T. Roorkee, who were always ready to help and suggest when I got stuck up at any stage during the tenure of experimentation.

I wish to record my deep sense of gratitude to the Head, Centre of Nanotechnology, Dr. Anil Kumar to provide necessary material for the successful completion of the experimentation, and Head, IIC, Indian Institute of Technology, Roorkee, for extending necessary facilities during the experimental work.

I thank my friends and classmates, who continuously helped and supported me during the entire stay of two years in IIT Roorkee, making it a memorable phase of my life.

I sincerely and gratefully acknowledge the moral support, blessings and continuous encouragement from my parents and family members throughout the period of my work.

Finally, I am grateful to God for giving me strength and patience for the successful completion and timely submission of the thesis.

<div align="right">

GYANAVI

</div>

ABSTRACT

Sol-gel technology for Hydroxyapatite (HAp) synthesis has been developed more than a decade ago. The existing sol-gel HAp synthetic methods which use alkoxide - based precursors require solvent based diluting media, a moisture – controlled atmosphere, prolonged synthesis time generally greater than 24 hours, and a heat treatment at temperature greater than 500°C over a time period of several hours. Those limit practical applications of HAp. Therefore, in this work, HAp ceramics were synthesized using water based sol – gel route with Calcium nitrate and Triethyl phosphite as calcium and phosphorous precursors, respectively. It was expected that the water based sol – gel process can be a feasible materials technology for biomedical applications. Water was the only medium used as diluting medium for HAp sol preparation. The sol only became gel after the removal of solvent at 80°C. XRD showed that the apatitic structure first appeared at a temperature as low as 400°C. The XRD analysis was used to examine the phase transformation of HAp at different temperature. The functional group change of HAp at different temperature was observed by FTIR spectroscopy. The morphological feature of the raw and sintered samples was examined. The synthesized powder was characterized through FTIR, XRD, Thermal analysis and SEM analysis.

CONTENTS

LIST OF FIGURES

LIST OF TABLES

CHAPTER 1

INTRODUCTION

Apatites have the general formula $Ca_{10}(PO_4)_6X_2$, where X is commomly F or OH. They form an important series of minerals, as most of the world's supply of phosphorous for the fertilizer and other industries comes from the apatite deposits with a composition close to Fluorapatite $Ca_{10}(PO_4)_6F_2$. On the other hand, hydroxyapatite is a rare mineral, but it is the most important calcium phosphate in the animal kingdom because it is closely related to the basic calcium phosphate present in teeth and bone.

Calcium phosphate ceramics were first proposed by Albee and Morrison in 1920 for biomedical applications. They observed that tricalcium phosphate, injected into defects, demonstrated more rapid bone growth and union than the untreated defects. Hydroxyapatite (HAp) was first identified as being them mineral component of bone in 1926 by DeJong. However, it was not until about 25 years ago that synthetic hydroxyapatite [$Ca_{10}(PO_4)_6(OH)_2$] was accepted as a potential biomaterial for use in orthopaedics, bone grafts and dentistry [1]. Calcium phosphate ceramics, particularly those with Ca/P ratio between $1.5 - 1.67$, i.e. tricalcium phosphate and stoichiometric hydroxyapatite respectively, have long been used as prime candidate biomaterials to reconstruct, restore, and replace human bone. This is because of their close similarity with the mineral found in calcified tissues, such as bone, tooth enamel and dentine, in humans and vertebrates. Hydroxyapatite is one of the most important calcium phosphates and have received wide attention as bone substitutes over the past few decades [28][29][30]. One remarkable property of HAp is its close resemblance in chemical and crystallographic structute to that of the mineralized component in vertebrate teeth and bone. HAp has been the most widely studied calcium phosphate since it demonstrated excellent biological affinity to host tissue, by forming chemical bond at the implant-tissue interface. Natural one mineral is non-stoichiometric and contains HPO_4^{2-} and CO_3^{2-} groups that potentially replace the PO_4^{3-} and OH^- groups in the apatitic lattice, so its chemical composition could be formulated as

$Ca_{10-x}(PO_4)_{6-y}(HPO_4)_y(CO_3)(OH)_{2-x-y/3}$. Thus, naturally occurring apatite is essentially a carbonate-containing apatite and has a nanometer-sized, poorly crystalline feature where metabolic activity with respect to the surrounding physiological environment is higher than for conventional, synthetic, well-crystallized HAp. Osteoconductivity, i.e. the ability to "guide" the growth of the bone tissue, is one of the major biological functions of the HAp that has been observed in animal models. Osteoinducivity (the ability to "induce" the formation of the bone, even within soft tissues such as muscles) of HAp has been mentioned earlier [31]. All these provide an extremely strong rationale for the HAp as a strong candidate for biomedical applications. HAp is also a strong candidate for replacement, restoration, and the regeneration of defective or disordered bones or hard tissues due to traumatic and non-traumatic events. HAp offers several advantages over other synthetic or naturally occurring materials, such as autografts (hard tissues from humans), xenograft (hard tissue from animals), and synthetic substitutes like metals, polymers and ceramics. These include:

1) Easy to synthesize in large quantity and at low cost, in comparison with autografts.

2) No risk of disease transmission and host body rejection such as xenografts.

3) Negative wear or adhesive tissue response, e.g., side effects, in comparison with metals and polymers.

4) Superior biocompatibility and bioactivity to human tissues as compared to those structural ceramics such as Al_2O_3, ZrO_2 (which are classified as bioinert materials), although these ceramics exibit better mechanical properties [32].

Biological functions of synthetic HAp are largely determined by its particle size, morphology, crystallinity, and composition, which depend on the synthesis precursors and processing. It is known that bone is a composite material consisting of nanoscale mineral particles, i.e. biological apatite (length ca. 50 nm, breadth ca. 25 nm and thickness up to 4 nm) and a matrix of collagen fibres (50–70 nm in diameter). Nanocrystalline HAp (Nano HAp) would be more interesting than micro-sized HAp from a biological and medical viewpoint because

2

of its similarity to minerals in natural bone. Compared to conventional microscale HAp, which lacks phase purity and homogeneity, nano HAp offers the possibility to enhance the rate of bone-bonding formation and to have excellent mechanical properties due to its high surface area to volume ratio, superior chemical homogeneity and microstructural uniformity. Furthermore, nano HAp was shown to be able to inhibit the growth of certain kinds of cancer cells, such as liver, throat and bone cancer cells, while having little side effect on normal cells. The rate of HAp bonding to bone was demonstrated to be dependent not on the composition but on the release of calcium and phosphate ions from HAp, determining the development of implant-bone interfacial strength. Consequently, sufficient dissolution of calcium and phosphate species is necessary to form bone-like apatite and bone bonding [33]. Accordingly, it is desirable to produce HAp with Ca/P ratio in between 1.5 and 1.67, and structurally resesmbling that of natural apatite. Most of the existing synthetic strategies require high temperature treatment to develop well-crystalline HAp in bulk, particulate, or coating form. However, well-crystalline HAp may not be an advantage in terms of biological activity, such as bioresorption, as compared to natural biocrystals. In contrast, biocrystals are nano-crysatlline and also poorly-crystalline structure, and are developed under physiological environment. Therefore it is expected that the lower the temperature for the synthesis of apatite, the more the resemblance in microstructure to that of the natural apatitic structure would occur. With the advancement of materials technology, a soft chemical route, termed "sol-gel process", to synthesize HAp has been proposed since 1990 and received considerable attention till date. Sol-gel process has several advantages, i.e., lower processing temperature, greater chemical and physical homogeneity and wider shape-forming capability. Therefore it would favourable if the sol-gel route could be applied to the synthsis of HAp. It is therefore the main purpose of this work to employ sol-gel technique to synthesize HAp.

The common features observed from the other existing sol-gel HAp synthesis, were solvent-based diluting media and medium-to-elevated heat treatment temperature like 500°C-900°C, for a time period of several hours and prolonged sol preparation, e.g., 24 hrs were reported. Those processing features may cause

adverse effect such as environmental pollution and are energy and time consuming. Moreover, the high reactivity of the sol-gel powder allows a reduction of the processing temperature and degradation phenomena occurring during sintering. The major limitation of the sol-gel technique is linked to the possible hydrolysis of phosphates [34].

Therefore it is more desirable to employ a sol-gel synthesis process that enables HAp to be developed at relatively low temperatures, without causing adverse effect to the environment. Keeping these things in mind, an alternative sol-gel process, with water as the only diluting medium, lower synthesis temperature and shorter period of synthesis time, was employed and the resulting powder was characterized using several standard characterization techniques.

CHAPTER 2

LITERATURE REVIEW

Chemical and structural resemblances between the natural apatite (i.e. mineral component of the bone) and the synthetic HAp allow strong chemical bonding to occur at the material bone interface. This results in a strong fixation of HAp implants which is particularly critical over the early stage of post – implantation. The mineral phase in the natural bone consists mainly of ~ 70 wt% of poorly crystalline apatite and a small amount of carbonated apatite. The poorly crystalline HAp, such as naturally occurring apatite, is prone to be more soluble in the physiological environment than the highly crystalline HAp which is commonly considered to be non – resorbable. However, due to brittleness of pure synthetic HAp ceramics, either composites or coating applications are frequently employed.

2.1 HAp STRUCTURE:

The similarity in crystallographic structure between bone mineral and Hydroxyapaite (HAp) was first observed by Dejong in 1926. Later, a refinement of the spatial arrangement of the constituent groups of Ca^{+2}, PO_4^{-3}, and OH^- ions in HAp crystal was further given by Posner et al. HAp has a hexagonal symmetry and the HAp unit cell is a right rhombic prism with a length along each edge of the basal plane of the cell of a ≈ 0.9423 nm and a height of c ≈ 0.6875 nm.

c plane
(PO₄ site: negative charge)

a plane
(Ca site: positive charge)

9.423Å

6.875 Å

C

a

a

OH   PO₄   Ca
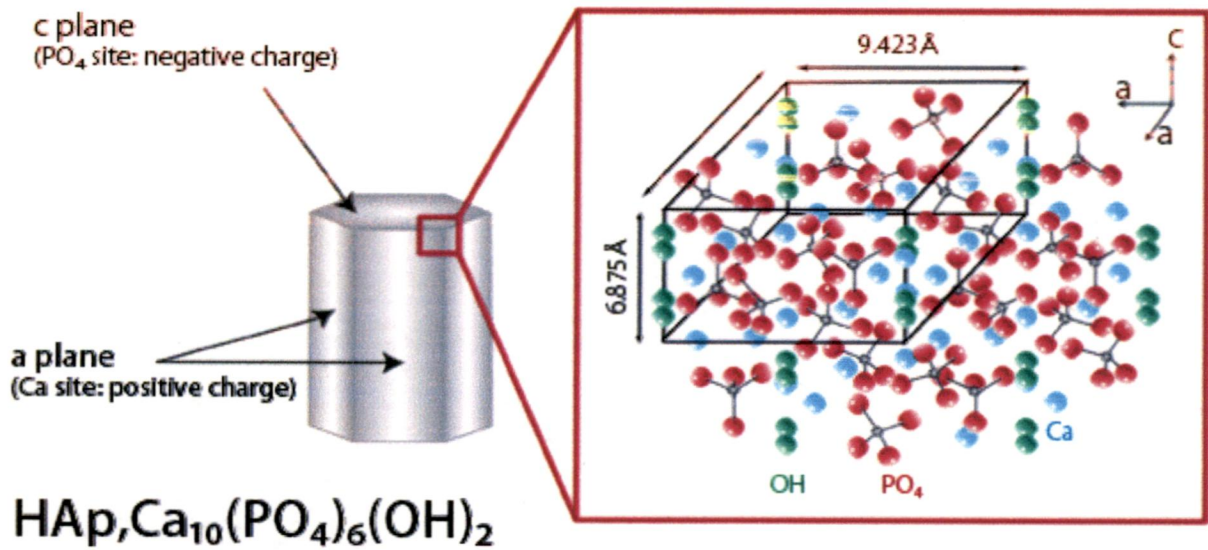
HAp, $Ca_{10}(PO_4)_6(OH)_2$

Fig. 2.1 structure of Hydroxyapatite molecule [35]

Pure stoichiometric HAp [$Ca_{10}(PO_4)_6(OH)_2$] consists of Ca^{2+}, PO_4^{3-}, and OH^- ions. The lattice structure is shown in figure with Ca^{2+} ions forming column structures and OH^- ions residing inside the channels.

● Ca
○ OH
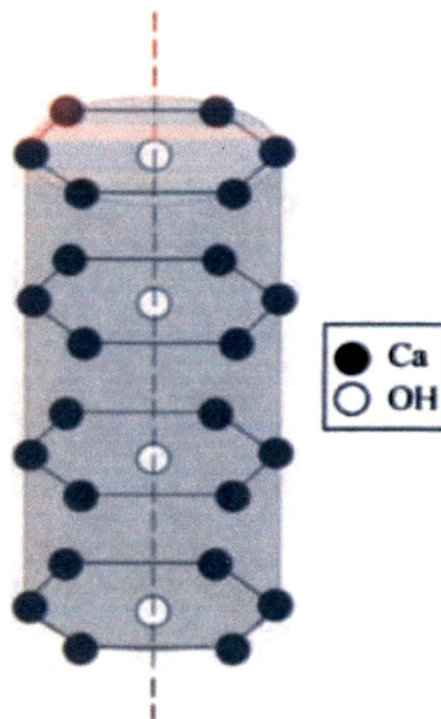
Fig. 2.2 The simplified lattice structure of apatite [10]

The structure of HAp belongs to Hexagonal system with a $P6_3/m$ space group. The overall arrangement of HAp is characterised by a c — axis perpendicular to 3 equivalent a-axis at angle 120° to each other. The unit cell, the smallest building unit and a complete representation of the HAp crystal, consist of a Ca^{2+}, PO_4^{-3} and OH⁻ groups closely packed together in a Hexagonal arrangement as shown in figure.
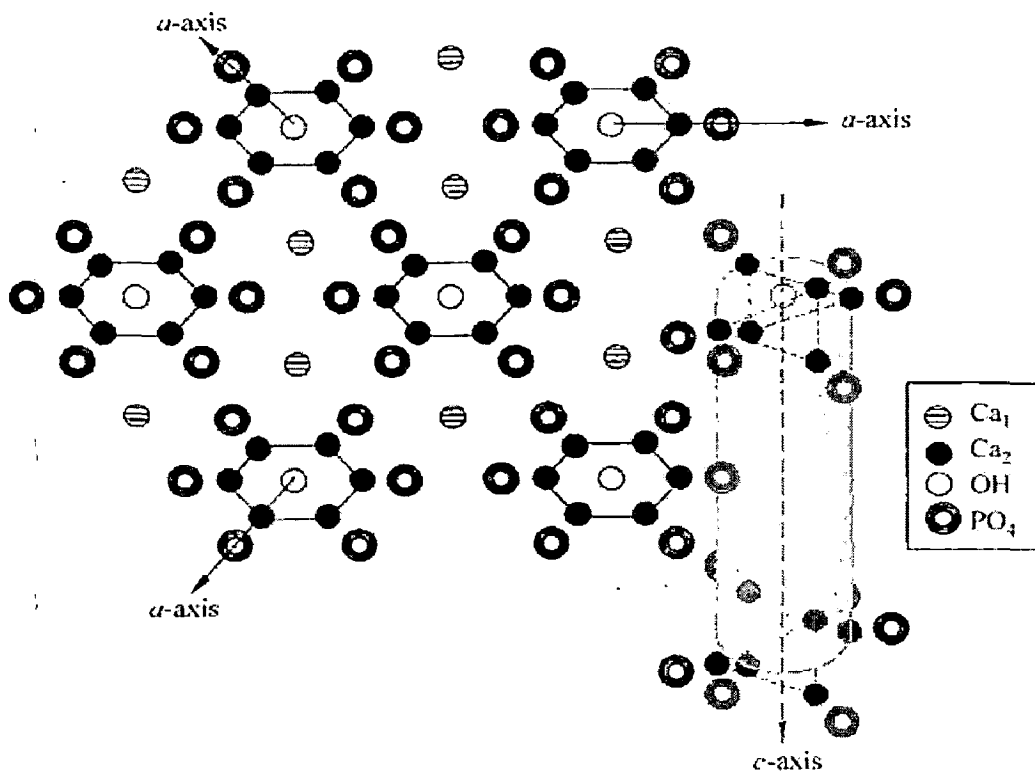
Fig. 2.3 the atomic arrangement of Calcium hydroxyapatite [10]

According to the position in the unit cell, 10 Calcium (Ca) atoms can be classified into 2 types : Ca_1 and Ca_2. Four calcium atoms occupy the Ca_1 positions, which locate in an octahedral site of a hexagonal array, and six calcium

7

atoms live in Ca$_2$ position, which locates at the corners of the hexagonal column and surrounds the OH⁻ ions. However, six Ca$_2$ atoms are not in the same plane, each three arrange in triangle positions at z = 0.25 and z = 0.75. The OH⁻ ions are located in the centreline of the hexagonal channel. Similar to the six Ca$_2$ atoms, the six phosphates (PO$_4$) are in a helical arrangement from level z = 0.25 to z = 0.75 and arrange in two triangles as well. Phosphate group form a skeletal frame structural network, which provides structural stability for HAp. [10]

One important feature of the HAp structure is that it is easily subject to isomorphous substitution. Ca positions can be substituted by numerous divalent or trivalent cations. Some anions such as F⁻, Cl⁻, CO_3^{-2} etc, are also known to replace OH⁻ as well as PO_4^{-3} ions to form isomorphs. In bone apatite, cationic substitutions by ions, such as Mg, Sr, F, Pb, is limited in quantity. However, Carbonate substitution as it is the third most abundant ion in bone apatite.

## 2.2: CONVENTIONAL TECHNIQUES FOR HAp SYNTHESIS

A number of methods have been used for HA powder synthesis. Calcium phosphates can be synthesised by hydrothermal, solid state or wet chemical reactions . One of the earliest techniques developed for the synthesis of HAp involved the hydro-thermal conversion of fluoroapatite to HAp under a pressure 5000 p.s.i . and temperature range of 920 –1230 °C. HA as a final product may be preceded by the formation of intermediate products such as β-calcium pyrophosphate or calcium monohydrogen phosphate depending upon the applied temperature and pressure. Most biomaterial applications use HAp prepared via the wet chemical method involving an aqueous solution of Ca salts and phosphates. Different calcium phosphates will precipitate from the system depending on its pH values. In order to obtain the required Ca/P ratio phase, this method usually needs long time (days) for complete reaction. The precipitated powder is usually calcinated at 400 – 600 °C or even at 1200 °C. However, fast precipitation during phosphate titration leads to chemical inhomogeneity in the final products. Slow titration and diluted solutions must be used to improve chemical homogeneity and stoichiometry of the resulting HAp, careful control of the solution condition is

critical in the wet precipitation. [11] other wise a decrease of pH below about 9 leads to the formation of Ca-deficient apatitic structure.

Another low temperature route of synthesis is by hydrolysis of some suitable calcium and phosphate precursors like dicalcium phosphate dihydrate [14] or beta tricalcium phosphate in water containing environment, the resulting HAp showed good crystallinity.

The solid- state synthesis of HAp from oxide or inorganic salt powders usually requires extensive mechanical mixing and lengthy heat treatments at high temperatures. These processing conditions, however, do not allow facile control over micro-structure, grain size and grain size distribution in the resulting powders or shapes.[12]

HAp is inherently brittle and shows relatively poor mechanical strength, which restricts its applications to the areas which require no or low load bearing ability like mandibular and maxillary augmentation, etc. A number of techniques are employed to fabricate HAp composites with secondary reinforcements such as metallic substrates (Ti, Ti-6Al-4V, 316 Stainless steel etc.) by coating. By taking advantage of the superior mechanical properties of biocompatible metals and the bioactivity of the HAp, the implants have been successful commercially and clinically, as well, for many years.[11]

2.3: SOL-GEL HAp SYNTHESIS

2.3.1: Process overview

Sol-gel synthesis of HAp ceramics has recently attracted much attention. The first alkoxide based sol-gel method to form HAp powder using calcium diethoxide and triethyl phosphate as precursors was utilised by a research group in Japan in 1990. The sol-gel method offers a molecular- level mixing of the calcium and phosphorus precursors, which capable of improving extent, in comparison with conventional methods. [13][15] Besides, the so-gel approach provides significantly milder conditions for the synthesis of HAp powders or films. In the sol-gel

synthesis of HAp, calcium alkoxides or salts are frequently used as calcium precursors. In most cases, phosphorus compounds – oxide, triethylphosphate and triethylphosphite are employing as phosphorus precursors in water or organic solvents phase. However a long period of the sol-gel preparation time, 24 h or longer is commonly reported in literature as required to form desirable product. This is because of slow reaction between calcium and phosphorus precursors in the sol phase. Obviously, the reactivity depends on the chemical nature of the precursors. Phosphate esters, being very stable towards water, can not be hydrolyzed easily and the hydrolysis may be possible in the presence of metal ion-containing catalysts. The phosphate esters have the larger hydrolysis rate constants, than corresponding phosphate esters compounds[15]
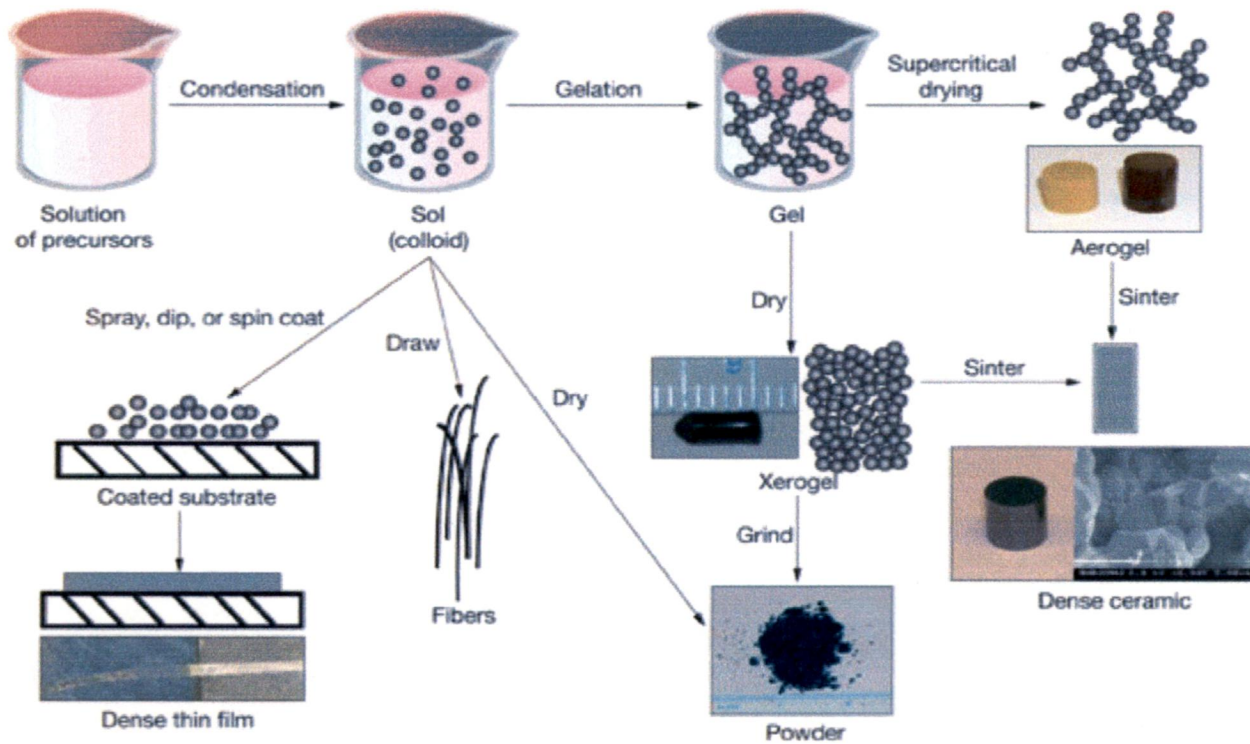

Fig 2.4 The sol-gel process [36]

The versatility of sol-gel method opens a great opportunity to form thin film

coatings and has currently being widely used for biomedical applications.[16] The sol-gel process provides much milder conditions for HAp thin films synthesis. This results in much better structural integrity whereas the defects caused during plasma spraying can be avoided [16]. Also the lower temperature synthesis of HAp thin films particularly benefits the metal implant substrate where the mechanical degradation or the phase transition of the underlying alloy can be prevented. However, thermal treatment of HAp sol-gel films in vacuum is frequently required to avoid metal oxidation. This leads to structural instability of HAp coating (i.e. evolution of structural water) during vacuum thermal treatment. Therefore from both economic and practical points of view, thermal treatment of HAp coating should be performed in air [9]. The primary focus was a low temperature sol-gel synthesis of HAp. Recently HAp has been used as a vehicle for drug delivery.[18][19][20].

Many combination of precursors for calcium and phosphorous were employed for sol-gel HAp synthesis. For example, Gross et al. used calcium diethoxide and triethyl phosphate to form pure HAp phase at temperature above 600°C [21]. They also found that ageing time longer than 24 h is critical for the solution system such that a monophasic HAp can be produced [22]. Otherwise large weight loss during pyrolysis and undesirable phases like CaO, could be observed. Jillavenkatesa et al. [23] synthesized a mixture of HAp and CaO at a temperature of 775°C using calcium acetate and triethyl phosphate as precursors. A further HCl leaching was required in that process to remove the CaO and to obtain pure phase of HAp. Brendel et al. [24] obtained HAp at a temperature as low as 400°C using calcium nitrate tetrahydrate and phenyldichlorophosphite as precursors. But the resulting HAp was of low purity and poor crystallinity. Further sintering of the sample resulted in better crystallinity. Kuriakose et al. [25] developed a sol-gel route to synthsize nanocrystalline stoichiometric hydroxyapatite by using calcium phosphate and ammonium phosphate precursors in ethanol medium at a temperature of 85°C . The resulting powder was stable and monophasic. Chai et al. [15] used calcium diethoxide and triethylphosphite in ethanol media to prepare nanocrystalline HAp thin film after ageing period of 7 days.

Haddow et al. [26] used calcium acetate together with a number of phosphorous precursors, namely phosphoric acid, phosphorous pentaoxide, and triethyl phosphite for coating applications. They found that the film prepared from triethyl phosphite and calcium acetate showed the best wetting characteristics and the temperature required to form an apatitic phase was greater than 600°C. Weng et al. [27] synthesized HAp using a mixed ethanol solution of calcium nitrate and phosphorous pentaoxide. A highly crystalline HAp coating with dense morphology was obtained after heat treatment at 500°C for 12-24 hours.

Phosphorous alkoxides have frequently been used as the phosphorous precursor for sol-gel synthesis of HAp in recent past. Triethyl phosphate and triethyl phosphite are the most commonly used among them [15,21,23,26]. The hydrolysis activity of triethyl phosphate is relatively poor and a higher solution temperature together with a prolonged time period (over several days) is needed to form HAp phase [23]. Alternatively triethyl phosphite offers much higher activity of hydrolysis [28] and recent study by means of P^{31} NMR revealed a valence transition from P(III) to P(V) upon ageing with calcium precursor to form HAp within 24 hrs [21]. This indicates a nucleophilic addition of negatively charged OH⁻ groups to the positively charged metal P, leading to an increased co-ordination number of the phosphorous atom which is essentially an indication towards the polymerization reaction [28]. After subsequent protonation of the alkoxide ligand (-OR) and removal of the charged ligand (-OR)⁺, P-(OR), following interaction with Ca precursor to develop the aptitic structure [29].

Besides the difference in the chemical activity of the precursors, such as hydrolysis, polycondensation, etc. the temperature that is required to form the apatitic structure depends largly on the nature of the precursors. The sol-gel process parameters vary considerably for synthesis of phase pure HAp. However, lower-temperature, environment-friendly, and shorter processing time are currently most desirable for the sol-gel synthesis. Therefore a water-based, low-temperature synthesis of the HAp is the focus of this work.

Table 1: Chemical precursors, solvents and the synthetic parameters for various sol-gel HAp synthesis processes

Chemicals	Solvent	Temperature	Time	Reference
Ca(NO₃)₂ C₆H₅PCl₂	Ethanol	>500°C	---	T. Brendel, 1992 [24]
Ca(OEt)₂ P(OPr)₃	Ethanol	500°C	24 hrs	C.S. Chai, 1995 [1]
Ca(OEt)₂ PO(OEt)₃	Ethanol	>600°C	>24 hrs	K.A. Gross, 1998 [21]
Ca(C₂H₃O₂)₂ PO(OEt)₃	Water	>775°C	>48 hrs	Jillavenkatesa, 1998 [23]
Ca(C₂H₃O₂)₂ H₃PO₄/P₂O₅/P(OEt)₃	Ethanol	>600°C	----	D.B. Haddow, 1998 [26]
Ca(NO₃)₂ P₂O₅	Ethanol	500°C	48 hrs	W. Weng, 1998 [27]
Ca₃(PO₄)₂ (NH₄)₃PO₄	Ethanol	85°C	-----	T.A. Kuriakose, 2004 [25]

2.3.2: Hydrolysis of Sol-Gel HAp precursor

In conventional sol-gel synthesis, metal alkoxides are frequently used as the starting materials. In this process the alkoxides are hydrolysed in the presence of water, hydroxyl groups nucleophilically substitute alkyl groups bonded to the metal atom (M) and alcohol molecules (ROH) are released as by-product:

$$M - (OR) + H_2O \rightarrow M - (OH) + ROH \tag{2.1}$$
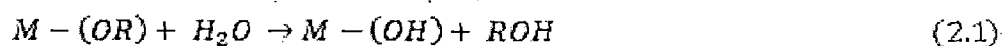
A subsequent polymerization-condensation reaction between M-(OH) molecules leads to the formation of -M-O-M- bond and water as by-product:

$$M - (OH) + M - (OH) \rightarrow M - O - M + H_2O \qquad (2.2)$$
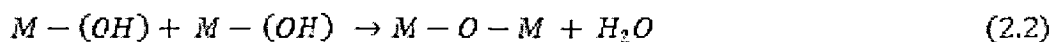
Reaction (2.1) and (2.2) can be accelerated by acid or base catalyst. For most sol-gel glasses/oxides, reaction (2.2) proceeds spontaneously at room tempareture to form a thre dimensional structure, resulting in a solid like gel. However, for orthophosphates, reaction (2.2) requires a moderate heat treatment to solidify the 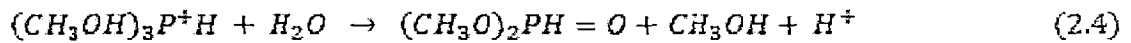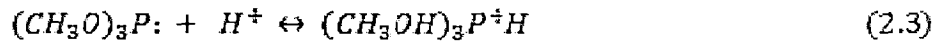sol solution [30,31]. A few examples demonstrated gelation of the orthophosphates at ambient environment if calcium ethoxide [32] or calcium glycolate [33] was employed as a starting material under highly acidic conditions.

A number of combinations between calcium and phosphorous of various chemical forms have been adapted for HAp formation, as presented in Table 2.1. Triethyl phosphite has most widely been used as one of the precursors because of its rapid hydrolysis, as opposed to trialkyl phosphate precursor. Subsequent interaction of the hydrolyzed phosphite with calcium precursors, for example, calcium ethoxide [32], calcium acetate [23], or calcium-acetate-glycolate [33], proceeds slowly to form Ca-P containing derivatives. During the reactions, an increase in the co-ordination number of the phosphorous from (III) to (V) was detected through P^{31} NMR, an evidence of polymerization [21,28,32]. Non-aqueous solvents are frequently employed for dilution of triethyl phosphite, together with a small amount of water or acetic acid for hydrolysis.

Triethyl phosphite is immiscible with water and forms emulsion phase after mixing with water. The emulsion transforms into a clear solution after a certain period of time, then the phosphite odour disappears, indicating a complete hydrolysis. Westheimer et al. [28] proposed that the trialkyl phosphite proceeds rapidly to form dialkyl phosphate in acid. For instance, in the case of trimethyl phosphite, the unshared electron pair in trimethyl phosphite will react rapidly with proton to form protonated phosphite, followed by deprotonation to form a product:

14

$$(CH_3O)_3P: + H^+ \leftrightarrow (CH_3OH)_3P^+H \qquad (2.3)$$

$$(CH_3OH)_3P^+H + H_2O \rightarrow (CH_3O)_2PH = O + CH_3OH + H^+ \qquad (2.4)$$

However chemistry of extended hydrolysis of dimethyl or diethyl hydrogen phosphite has not been fully identified . according to the reactions proposed by Masuda et al. [32], diethyl hydrogen phosphite underwent further hydrolysis or chemical modification to form monoethyl phosphite, followed by interaction with Ca to form a complex containing Ca and P. Crystalline HAp then developed after heat treatment of the chemical complex at > 600°C.

It is known that polymerization reaction usually accompanies hydrolysis. Therefore, a reaction to form oligomeric phosphorous compound during synthesisis possible. This would result in the formation of calcium phosphate material other than HAp and accordingly, having a lower Ca/P ratio than stoichiometric HAp.

2.3.3: Ageing of the sol-gel HAp

In sol-gel synthesis of HAp, alkoxides or metal salts are frequently used either as calcium or phosphorous precursors. In most of the cases, phosphorous alkoxides were employed as one of the major constituents, together with stoichiometric amount of calcium alkoxide or calcium salts to form HAp. However, a long sol preparation time, eg. 24 hrs or more, is commonly reported in order to form a desirable product (refer to Table 1). this is because of the slow reaction of calcium and phosphorous precursors in the sol phase. Obviously the activity depends on the chemical nature of the precursors, for example, it took at least 24 hrs for the most often used, highly active phosphorous alkoxide, triethyl phosphite, to interact with calcium alkoxide in order to obtain HAp [21,34]. In the case of less active triethyl phosphate longer time and higher temperature treatment

is necessary to activate the interaction with calcium acetate to form crystalline HAp [23]. The details of the chemical pathways is not clearly understood in any case and the chemical reactions proposed may be oversimplified in terms of "real" reactions [32,33].

2.3.4: Structural evolution of sol-gel derived HAp

Low temperature formation of the apatitic crystal has been the main advantage of the sol-gel process in comparison to the other conventional methods. Higher temperatures usually more than 1000°C are required to sinter the apatitic crystals formed by wet precipitation process, while 700-900°C temperature is required ot densify sol-gel derived HAp powder [1]. Moreover sol-gel HAp has a finer grain structure which is better accepted by the host tissue. Several days are needed to complete the hydrolysis reaction of the phosphorous precursor and a subsequent reaction with Ca precursor is critical in developing a desirable apatitic phase. A specific ageing time either at ambient temperature or higher temperature is necessary to form phase-pure apatitic structure. Insufficient ageing causes formation of impurity phases like Calcium oxide or Calcium carbonate, which suggests incomplete reaction between hydrolysed phosphate precursor and the calcium precursor [22,34]

CHAPTER 3

OBJECTIVES AND SCOPE

3.1: Objectives

The general objective of this work was:

1) To utilize the sol-gel technique to synthesize HAp bioceramics material, having

following characteristics:

(i) Sol preparation under ambient environment.

(ii) Use of water as the only diluting medium for calcium and phosphorous

precursors.

(iii) HAp synthesis at a temperature below 500°C.

2) To study the effect of sintering temperature on phase evolution of HAp.

3) To study the effect of sintering temperature on the microstructure of HAp material.

4) To study the thermal behaviour of the HAp material.

5) To study the effect of sintering temperature on crystallite size and lattice parameter

of the synthesized HAp material.

3.2: Scope

In this work, Triethyl phosphite $P(OC_2H_5)_3$, and Calcium nitrate tetrahydrate $Ca(NO_3)_2.4H_2O$, were used as phosphorous and calcium precursors respectively for synthesizing HAp by sol-gel process. Processing parameters that are critical to

resulting HAp included sintering temperature, hydrolysis time and ageing time. The range of these parameters is as follows,

1) Tempearture: 400-1200°C

2) Heat treatment environment: Ambient

3) Hydrolysis time: very short, a few minutes

4) Ageing time: 24 hrs

As a result, HAp was achieved with phase composition having phase pure hydroxyapatite with Ca/P ratio in the vicinity of stoichiometry, 1.67. The crystallinity of the resulting HAp should be controllable, for example from poorly-crystalline to well-crystalline HAp.

The resulting HAp was further characterized in terms of microstructure using Field effect scanning electron microscopey (SEM), elemental analysis and Ca/P ratio by Energy Dispersed Spectroscopy (EDS), crystal phase via X-ray diffraction analysis (XRD) and Fourier transform infrared spectroscopy (FT-IR), thermal behaviour using Thermogravimetric analysis (TGA) and Differential thermal analysis (DTA).

CHAPTER 4

EXPERIMENTAL TECHNIQUES

4.1 XRD Diffractometer

An X-ray diffractometer analyzes crystalline states under normal atmospheric conditions. This method is non destructive. X-rays focused on a sample fixed on the axis of the spectrometer (goniometer) are diffracted by the sample. The changes in the diffracted X-ray intensities are measured, recorded and plotted against the rotation angles of the sample. The result is referred to as the X-ray diffraction pattern of the sample. Computer analysis of the peak positions and intensities associated with this pattern enables qualitative analysis, lattice constant determination and/or stress determination of the sample. Qualitative analysis may be conducted on the basis of peak height or peak area. The peak angles and profiles may be used to determine particle diameters and degree of crystallization, and are useful in conducting precise X-ray structural analysis.
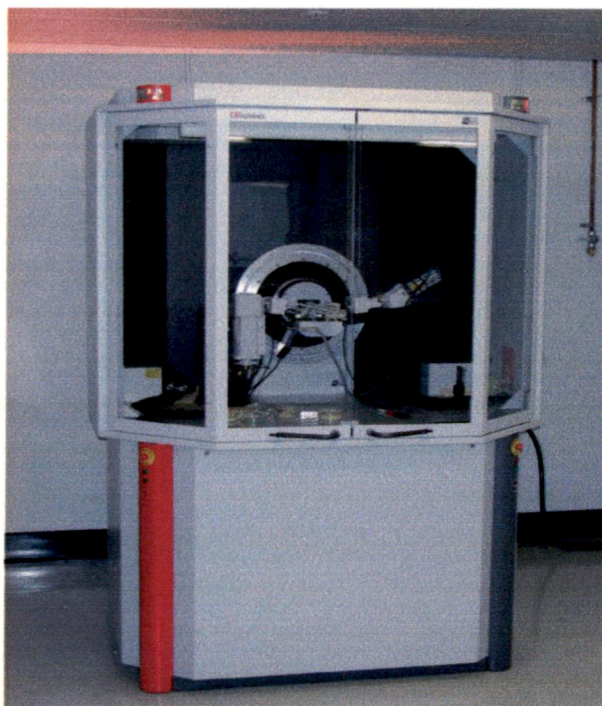
Fig. 4.1 X-ray powder diffractometer (Bruker D8 Advance)

The identification of single or multiple phases in an unknown sample is the main application of X-ray powder diffractometry.

When a monochromatic X-ray beam with wavelength lambda is projected onto a crystalline material at an angle theta, diffraction occurs only when the distance travelled by the rays reflected from successive planes differs by a complete number n of wavelengths.

4.1.1 Bragg's law

By varying the angle *theta*, the Bragg's Law conditions are satisfied by different *d*-spacings in polycrystalline materials. Plotting the angular positions and intensities of the resultant diffracted peaks of radiation produces a pattern, which is characteristic of the sample. Where a mixture of different phases is present, the resultant diffractogram is formed by addition of the individual patterns.

$$n\lambda = 2d \cdot \sin\theta$$
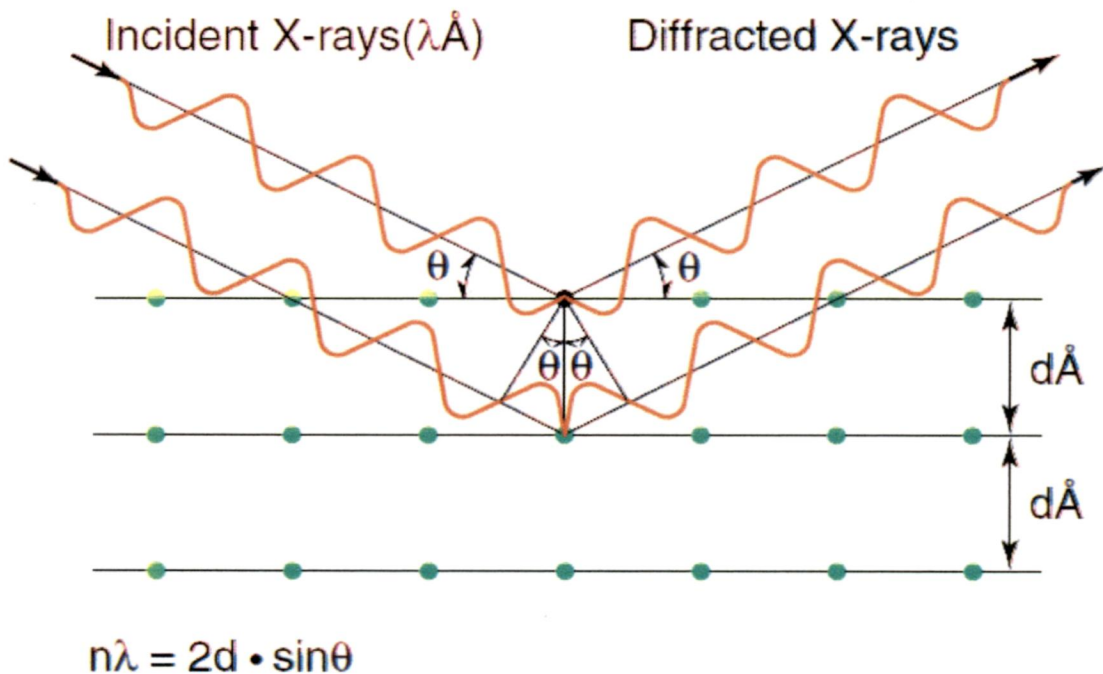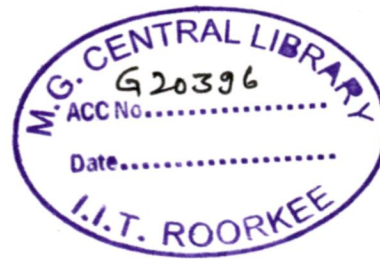
Fig. 4.2 Bragg's Law [37]
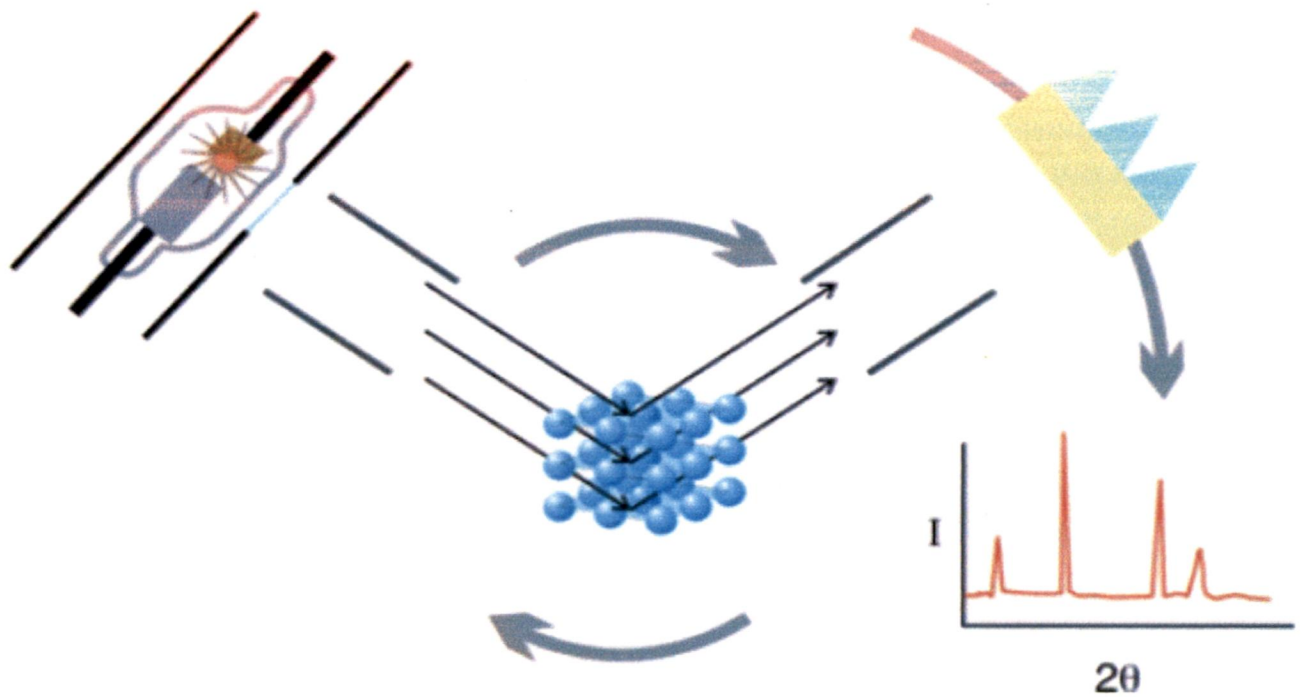
Fig. 4.3 Schematic representation of X-ray Diffractometer [37]

4.2 FESEM

FESEM stands for Field emission scanning electron microscope. The FESEM is a microscope that uses electrons instead of light to form an image. Since their development in the early 1950's, scanning electron microscopes have developed new areas of study in the medical and physical science communities. The FESEM has allowed researchers to examine a much bigger variety of specimens.

The scanning electron microscope has many advantages over traditional microscopes. The FESEM has a large depth of field, which allows more of a specimen to be in focus at one time. The FESEM also has much higher resolution, so closely spaced specimens can be magnified at much higher levels.

Because the FESEM uses electromagnets rather than lenses, the researcher has much more control in the degree of magnification. All of these advantages, as well as the actual strikingly clear images, make the scanning electron microscope one of the most useful instruments in research today.

4.2.1 Parts of FESEM

The sample is fixed with conductive tape (10) on a metallic sample block (11). Non-conductive specimen are coated with a nanometer thin-layer of metal to facilitate emission and flow of electron in the surface. The metal block is crewed on a sample holder (9) and positioned in the pre-vacuum chamber (7), an intermediate chamber with a front and a rear lid. This chamber acts as a lock. When the vacuum in this space is low enough, the shutter to the high vacuum (lowest pressure) is opened and the object is shifted with a long rod (8) into the object chamber on a rails just under the column (1). In order to ease the positioning of the sample, one can observe the inner view of the object chamber with an infrared camera. The object chamber is the place where the sample is irradiated by the electron beam. The position of the sample stage can be adjusted in height (z-navigation; 5) and horizontally (x-y navigation; 6). The topographical scanning electron imaging requires a secondary electrons detector (4), like in a normal SEM there is a control panel (13), a monitor for the operation of the device (15) and one showing the SE images (14). A separate EDS detector (3) allows one to capture the X-ray scanning and there is another back -scattered electron detector. In this chamber in the heart of the electron microscope the vacuum is extremely low: 10^{-6}mBar (thus 1:1.000,000,000 the normal atmospheric pressure; vacuum display = (16); around the electron gun the vacuum is even two orders of magnitude lower). The need for such extreme vacuum is that collision of bombarding electrons from the beam with gas molecules in the column would result in heat production. Cooling (18) and supply of electric power (19) are required in order to maintain this extreme vacuum.

Under vacuum, electrons generated by a Field Emission Source are accelerated in a field gradient. The beam passes through Electromagnetic Lenses, focussing onto the specimen. As a result of this bombardment different types of

22

electrons are emitted from the specimen. A detector catches the secondary electrons and an image of the sample surface is constructed by comparing the intensity of these secondary electrons to the scanning primary electron beam. Finally the image is displayed on a monitor.
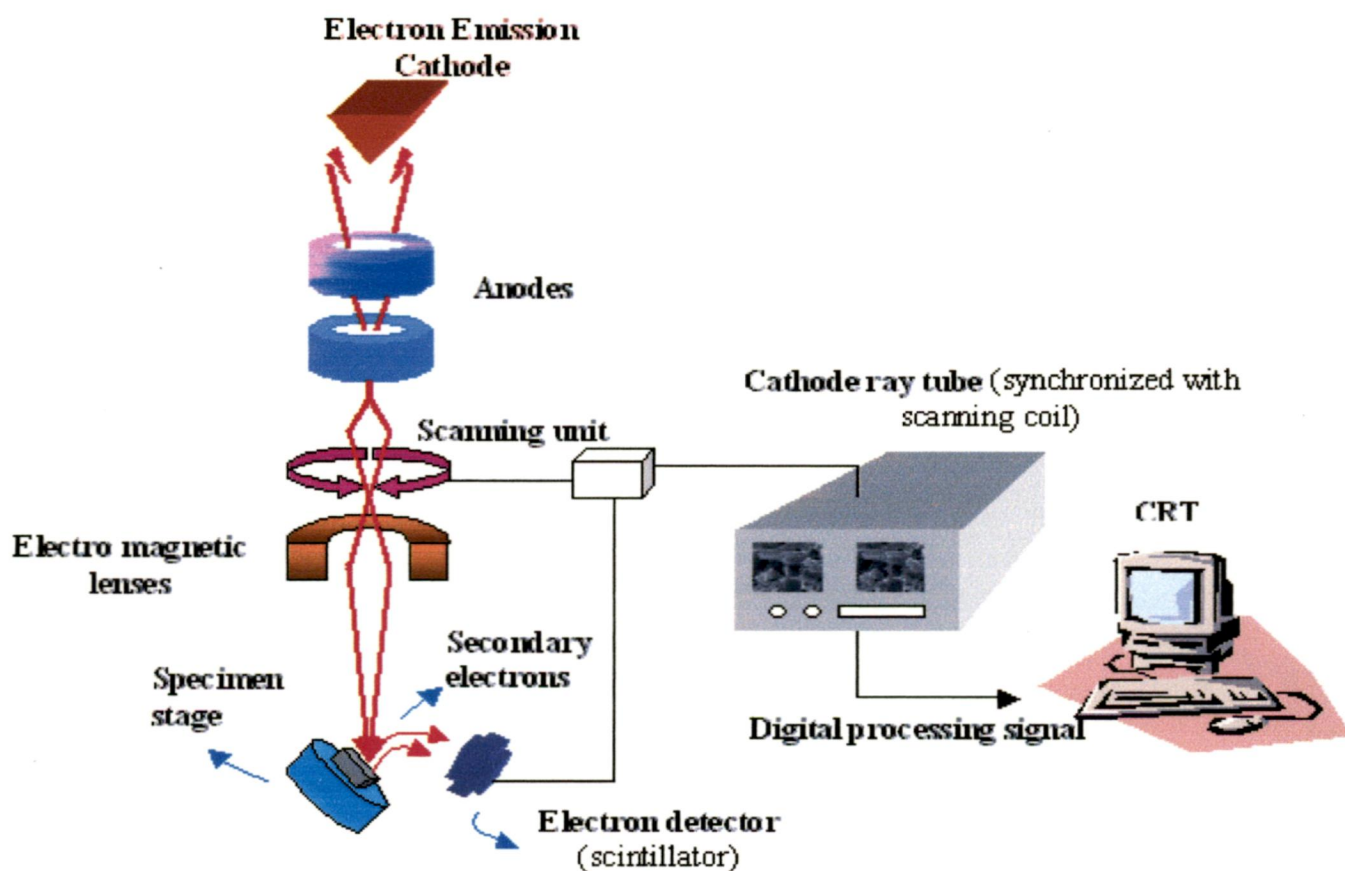
Fig. 4.4 *FESEM working principle*

4.2.2 Principle of FESEM

In FESEM the image is formed from secondary electrons that have been dislocated at the surface of the scanned sample by bombarding primary electrons from the electron gun. Those ejected electrons are captured by a detector and the information is converted into an electric signal, amplified and digitalized. The result is a topographical image of the *surface* of the object, e.g. the surface of a metal coating or lamellae of fish gills. Besides secondary electrons, radiation (in

particular X-rays and cathodoluminescence in typical samples) as well as back-scattered and so called Auger electrons with an own energy level are produced upon interaction of atoms in the surface layer of the sample with the primary electron beam. These emission signals, which contain information among others on the element composition of the upper layer, can be received by selected detectors, as is the case in EDAX microscopes for example, and combined with the topographical image.

Besides, there are scanning electron microscopes which are equipped with EDS (Energy Dispersed Spectroscopy) or EDAX (Energy-Dispersed Analysis of X-rays) detectors that capture the emitted X-ray (figure C, D and E). With such instruments it is possible to determine which elements are present in the surface layer of the sample (at a depth in the micrometer range) and where these elements are present ("mapping technique"). This particular microscope also allows one to capture directly reflected electrons, the so-called back scattered electrons (figure B), from which one can obtain a global appreciation whether one or several elements are present in the surface layer of the sample. Also the so-called Auger electrons, which are emitted just under the surface (F, G and H), provide information about the nature of the atoms in the sample.

A: The bombarding electrons (= primary electrons) can penetrate in the electron shells of the atoms composing the surface of the sample. The energy (negative charge, mass, velocity) of these incident electrons can be converted to eject local electrons, so-called secondary electrons, from the shells of the atoms in the surface of the specimen. This information can be utilized to reconstruct a detailed topographical image of the sample (SEI = Secondary Electrons Imaging). The final image looks like a shadow-cast photograph of the surface of the sample. This record of the morphology is the best known application of a scanning electron microscope.
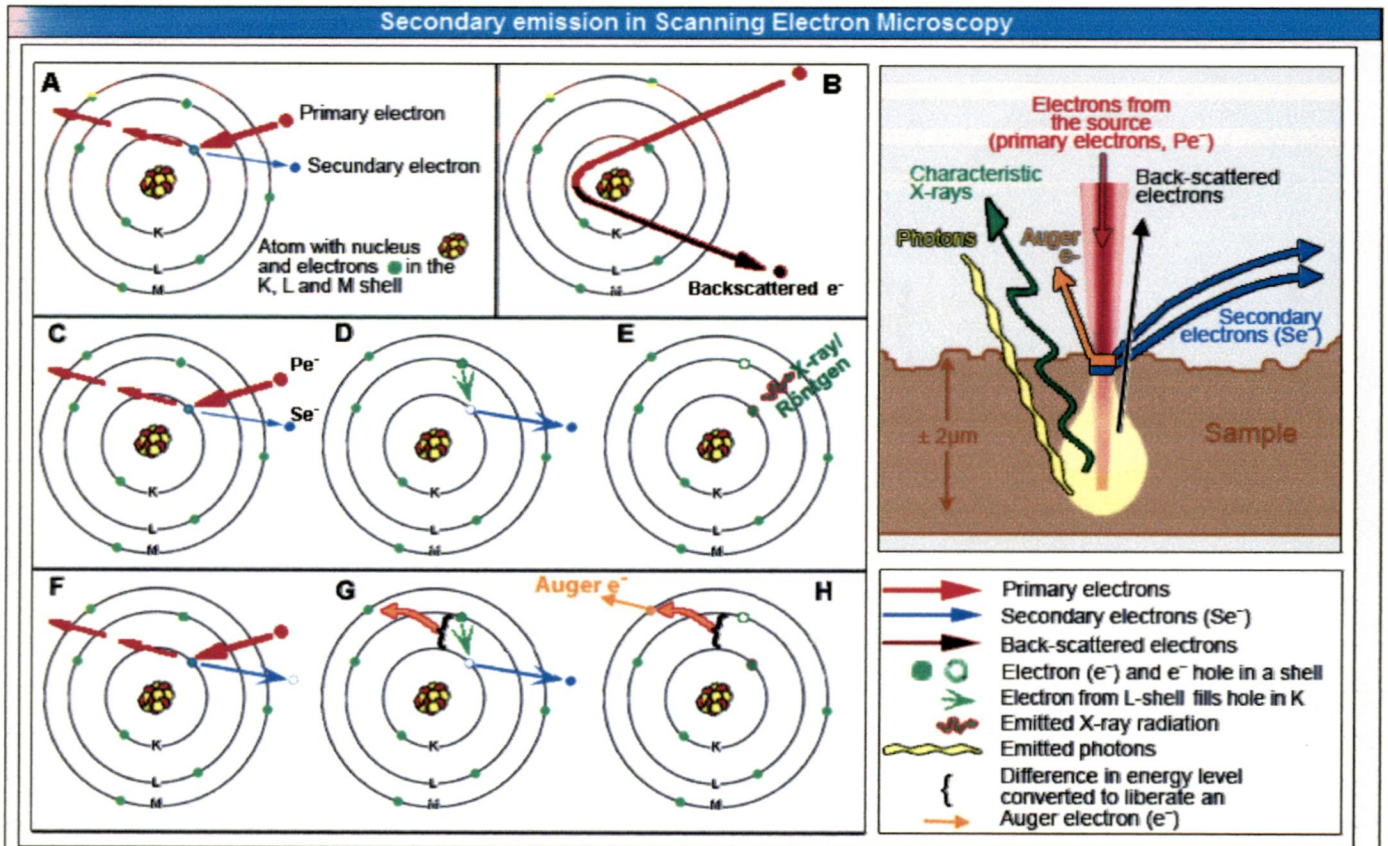
Fig. 4.5 Secondary emission in SEM

B: Primary electron can also be reflected by atoms at about 10-100 nanometre depth at the surface. These so-called "back-scatter" conserve their energy at incidence, but their direction of propagation has been modified upon interaction. One can obtain a rough representation whether the surface of the sample is constituted of a single or multiple element.

C, D, E: at the surface of the sample electrons in the deeper electron shells (shell K in C) can be ejected by primary electrons (Pe- indicated in red), resulting in an electron hole. When this lower-shell position is filled by an electron from a higher shell (green arrow in D) energy is released. This can be as light (photons; the phenomenon is also called cathode luminescence) or as X-ray. Because each element emits an own characteristic energy value, the elements present in the micrometer range depth of the sample can be determined.

F, G, H: another phenomenon is that the energy released upon filling a hole in the K shell by an electron from the L shell is used to expulse an electron from the external M shell: a so-called Auger electron. The released energy is

25

characteristic for the type of atom. Auger electrons are produced in the outermost surface layer (at nanometer depth) of the sample.

4.2.3 Sample Preparation

Because the SEM utilizes vacuum conditions and uses electrons to form an image, special preparations must be done to the sample. All water must be removed from the samples because the water would vaporize in the vacuum. All metals are conductive and require no preparation before being used. All non-metals need to be made conductive by covering the sample with a thin layer of conductive material. This is done by using a device called a "sputter coater."

The sputter coater uses an electric field and argon gas. The sample is placed in a small chamber that is at a vacuum. Argon gas and an electric field cause an electron to be removed from the argon, making the atoms positively charged. The argon ions then become attracted to a negatively charged gold foil. The argon ions knock gold atoms from the surface of the gold foil. These gold atoms fall and settle onto the surface of the sample producing a thin gold coating.

4.3 EDAX/EDS

Energy dispersive X-ray spectroscopy (EDS) is an analytical technique used for the elemental analysis or chemical characterization of a sample. It is one of the variants of XRF. As a type of spectroscopy, it relies on the investigation of a sample through interactions between electromagnetic radiation and matter, analyzing x-rays emitted by the matter in response to being hit with charged particles. Its characterization capabilities are due in large part to the fundamental principle that each element has a unique atomic structure allowing x-rays that are characteristic of an element's atomic structure to be identified uniquely from each other.

To stimulate the emission of characteristic X-rays from a specimen, a high energy beam of charged particles such as electrons or protons, or a beam of X-rays, is focused into the sample being studied. At rest, an atom within the sample

26

contains ground state (or unexcited) electrons in discrete energy levels or electron shells bound to the nucleus. The incident beam may excite an electron in an inner shell, ejecting it from the shell while creating an electron hole where the electron was. An electron from an outer, higher-energy shell then fills the hole, and the difference in energy between the higher-energy shell and the lower energy shell may be released in the form of an X-ray. The number and energy of the X-rays emitted from a specimen can be measured by an energy dispersive spectrometer. As the energy of the X-rays are characteristic of the difference in energy between the two shells, and of the atomic structure of the element from which they were emitted, this allows the elemental composition of the specimen to be measured.
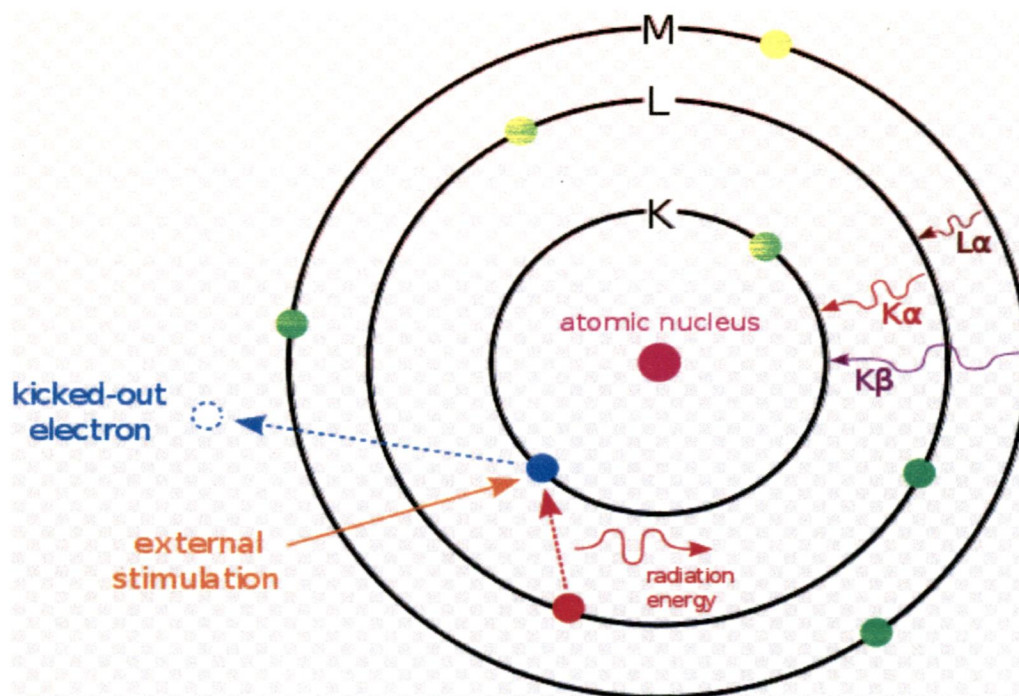

Fig. 4.6 Principle of EDAX

4.4 FT-IR

FT-IR stands for Fourier Transform Infra Red, the preferred method of infrared spectroscopy. In infrared spectroscopy, IR radiation is passed through a

sample. Some of the infrared radiation is absorbed by the sample and some of it is passed through (transmitted). The resulting spectrum represents the molecular absorption and transmission, creating a molecular fingerprint of the sample. Like a fingerprint no two unique molecular structures produce the same infrared spectrum. This makes infrared spectroscopy useful for several types of analysis.

Informations provided by FTIR:

> It can identify unknown materials

> It can determine the quality or consistency of a sample

> It can determine the amount of components in a mixture

Fourier Transform Infrared (FT-IR) spectrometry was developed in order to overcome the limitations encountered with dispersive instruments. The main difficulty was the slow scanning process. A method for measuring all of the infrared frequencies simultaneously, rather than individually, was needed. A solution was developed which employed a very simple optical device called an interferometer. The interferometer produces a unique type of signal which has all of the infrared frequencies "encoded" into it. The signal can be measured very quickly, usually on the order of one second or so. Thus, the time element per sample is reduced to a matter of a few seconds rather than several minutes. Most interferometers employ a beamsplitter which takes the incoming infrared beam and divides it into two optical beams. One beam reflects off of a flat mirror which is fixed in place. The other beam reflects off of a flat mirror which is on a mechanism which allows this mirror to move a very short distance (typically a few millimeters) away from the beamsplitter. The two beams reflect off of their respective mirrors and are recombined when they meet back at the beam splitter. Because the path that one beam travels is a fixed length and the other is constantly changing as its mirror moves, the signal which exits the interferometer is the result of these two beams "interfering" with each other. The resulting signal is called an interferogram which has the unique property that every data point (a function of the moving mirror position) which makes up the signal has information about every infrared frequency which comes from the source. This means that as the interferogram is measured, all frequencies are being measured simultaneously. Thus, the use of the interferometer results in extremely fast

28

measurements. Because the analyst requires a frequency spectrum (a plot of the intensity at each individual frequency) in order to make an identification, the measured interferogram signal can not be interpreted directly. A means of "decoding" the individual frequencies is required. This can be accomplished via a well-known mathematical technique called the Fourier transformation. This transformation is performed by the computer which then presents the user with the desired spectral information for analysis.

Sample analysis process:

The normal instrumental process is as follows:

1. The Source: Infrared energy is emitted from a glowing black-body source. This beam passes through an aperture which controls the amount of energy presented to the sample (and, ultimately, to the detector).

2. The Interferometer: The beam enters the interferometer where the "spectral encoding" takes place. The resulting interferogram signal then exits the interferometer.

3. The Sample: The beam enters the sample compartment where it is transmitted through or reflected off of the surface of the sample, depending on the type of analysis being accomplished. This is where specific frequencies of energy, which are uniquely characteristic of the sample, are absorbed.

4. The Detector: The beam finally passes to the detector for final measurement. The detectors used are specially designed to measure the special interferogram signal.

5. The Computer: The measured signal is digitized and sent to the computer where the Fourier transformation takes place. The final infrared spectrum is then presented to the user for interpretation and any further manipulation.
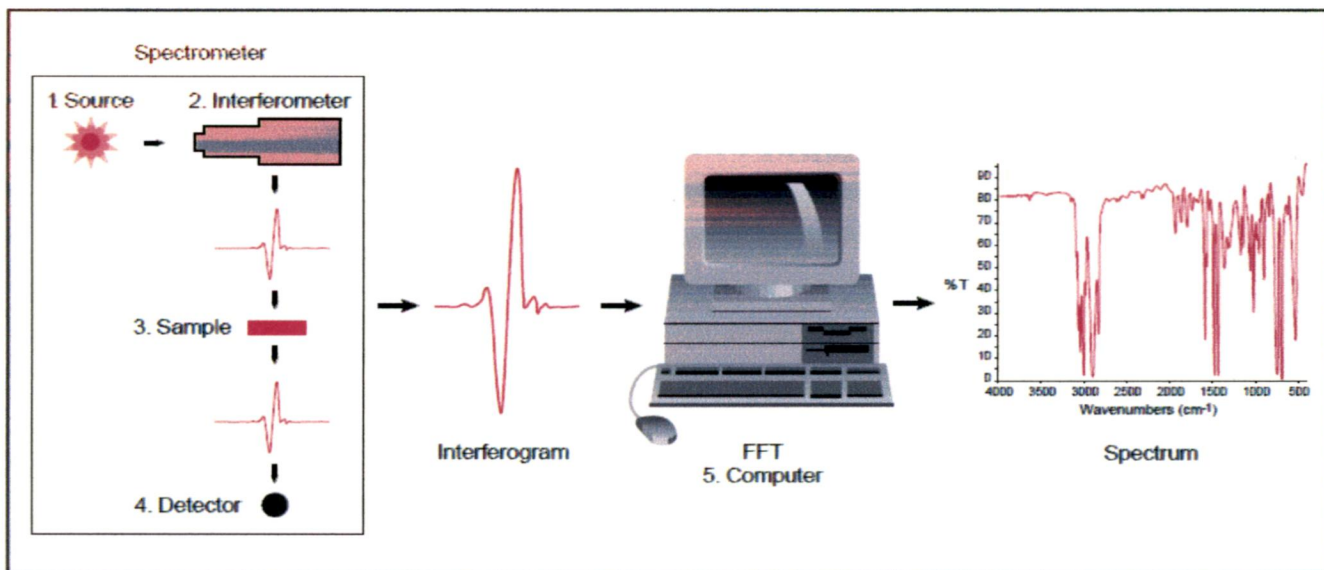
Fig. 4.7 FT-IR analysis process

Because there needs to be a relative scale for the absorption intensity, a background must also be measured. This is normally a measurement with no sample in the beam. This can be compared to the measurement with the sample in the beam to determine the "percent transmittance." This technique results in a spectrum which has all of the instrumental characteristics removed. Thus, all spectral features which are present are strictly due to the sample. A single background measurement can be used for many sample measurements because this spectrum is characteristic of the instrument itself.

Fig. 4.8 Layout of a Fourier transform infrared spectrometer

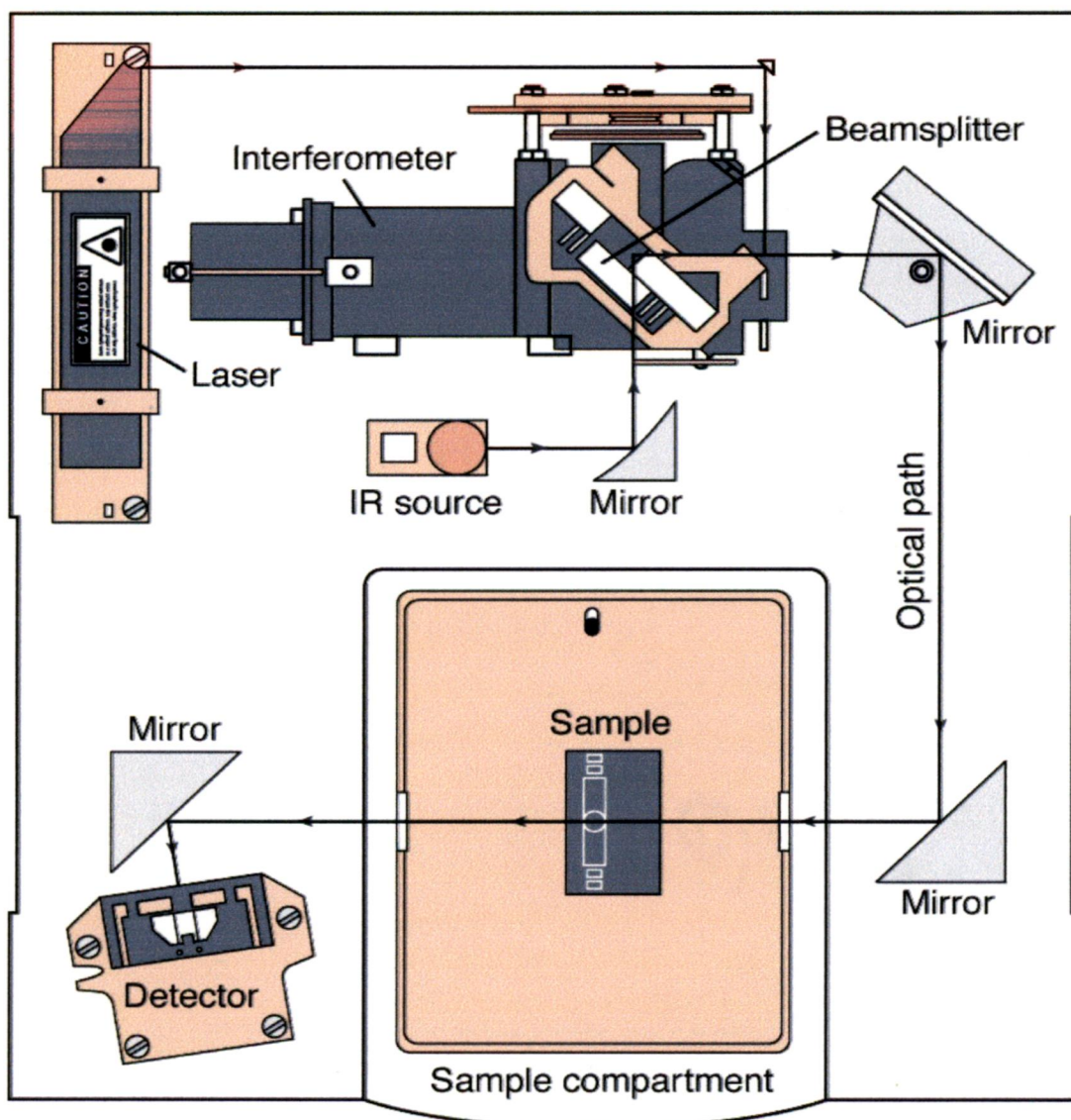## 4.5 Thermal analysis

Thermal analysis comprises a group of techniques in which a physical property of a substance is measured as a function of temperature, while the substance is subjected to a controlled temperature programme.

4.5.1 Thermogravimetric Analysis:

Thermogravimetric Analysis (TGA) is a technique in which the mass of a substance is measured as a function of temperature, while the substance is subjected to a controlled temperature programme.

Controlled temperature programme can mean:

- heating and/or cooling at a linear rate (by far commonest)
- isothermal measurements
- combinations of heating, cooling and isothermal stages
- other, more modern approaches, in which the temperature profile is modified according to the behaviour of the sample.
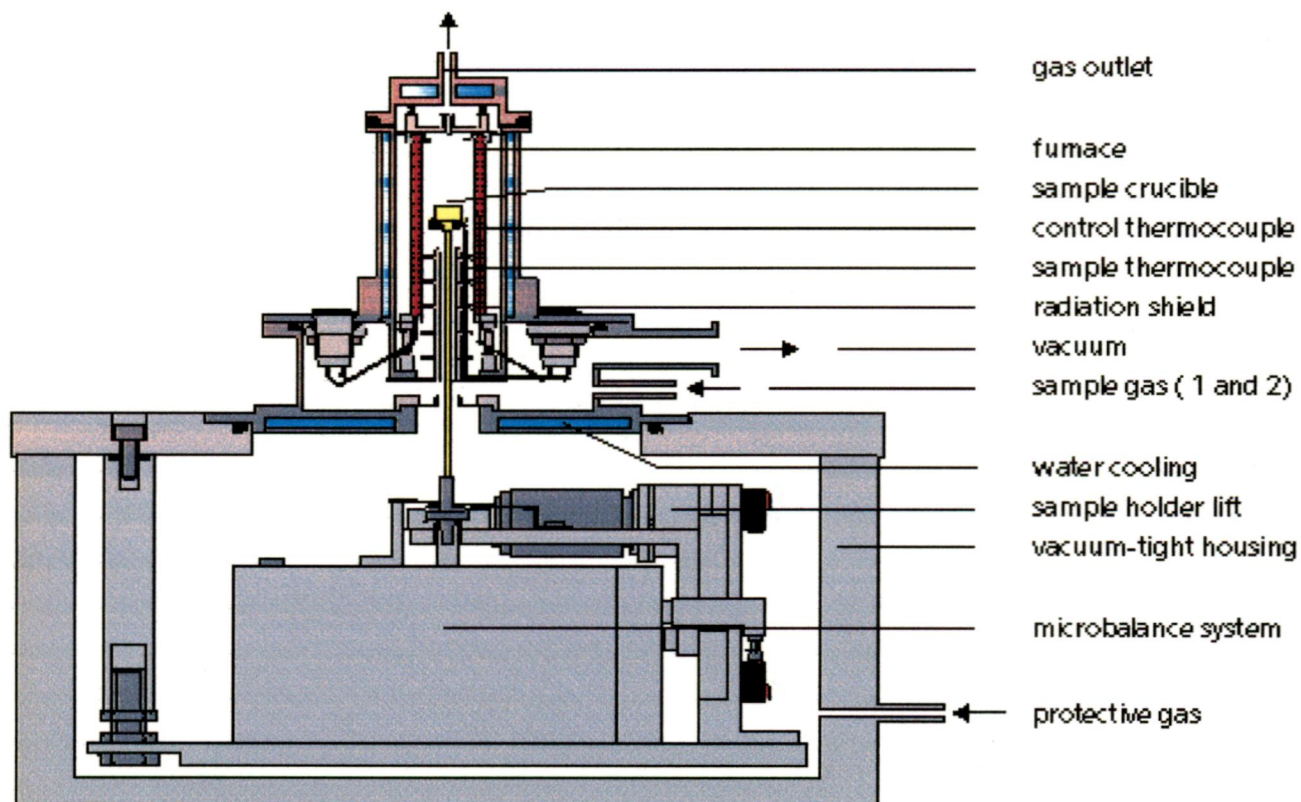

gas outlet

furnace
sample crucible
control thermocouple
sample thermocouple
radiation shield
vacuum
sample gas (1 and 2)

water cooling
sample holder lift
vacuum-tight housing

microbalance system

protective gas

Fig. 4.9 TGA apparatus

TGA is used primarily for determining thermal stability of polymers. The most widely used TGA method is based on continuous measurement of weight on a sensitive balance (called a *thermobalance*) as sample temperature is increased in air or in an inert atmosphere. This is referred to as *nonisothermal TGA*. Data are recorded as a thermogram of weight versus temperature. Weight loss may arise from evaporation of residual moisture or solvent, but at higher temperatures it results from polymer decomposition. Besides providing information on thermal stability, TGA may be used to characterize polymers through loss of a known entity, such as HCl from poly (vinyl chloride). Thus weight loss can be correlated with percent vinyl chloride in a copolymer. TGA is also useful for determining volatilities of plasticizers and other additives. Thermal stability studies are the major application of TGA, however.

A variation of the method is to record weight loss with time at a constant temperature. Called *isothermal TGA*, this is less commony used than nonisothermal TGA. Modern TGA instruments allow thermograms to be recorded on microgram quantities of material. Some instruments are designed to record and process DSC and TGA data simultaneously, and may also be adapted for gas chromatographic and/or mass spectrometric analysis of effluent degradation products.

4.5.2 Differential Thermal Analysis

A differential thermal analyser (DTA) measures the difference in temperature between the sample to be studied and an inert reference material as a function of temperature as both are subjected to the same temperature regime in a controlled environment heated or cooled at a controlled rate. The temperature difference is plotted against time or temperature. DTA measures the energy changes occurring on heating (or cooling) and enables enthalpies of reactions and phase changes to be obtained. Changes in the sample which lead to the absorption or evolution of heat can be detected relative to the inert reference.

Differential temperatures can also arise between two inert samples when their response to the applied heat treatment is not identical. DTA can therefore be used to study thermal properties and phase changes which do not lead to a change in enthalpy. The baseline of the DTA curve should then exhibit discontinuities at the transition temperatures and the slope of the curve at any point will depend on the microstructural constitution at that temperature.

A DTA curve can be used as a finger print for identification purposes, for example, in the study of clays where the structural similarity of different forms renders diffraction experiments difficult to interpret.

The area under a DTA peak can be due to the enthalpy change and is not affected by the heat capacity of the sample.
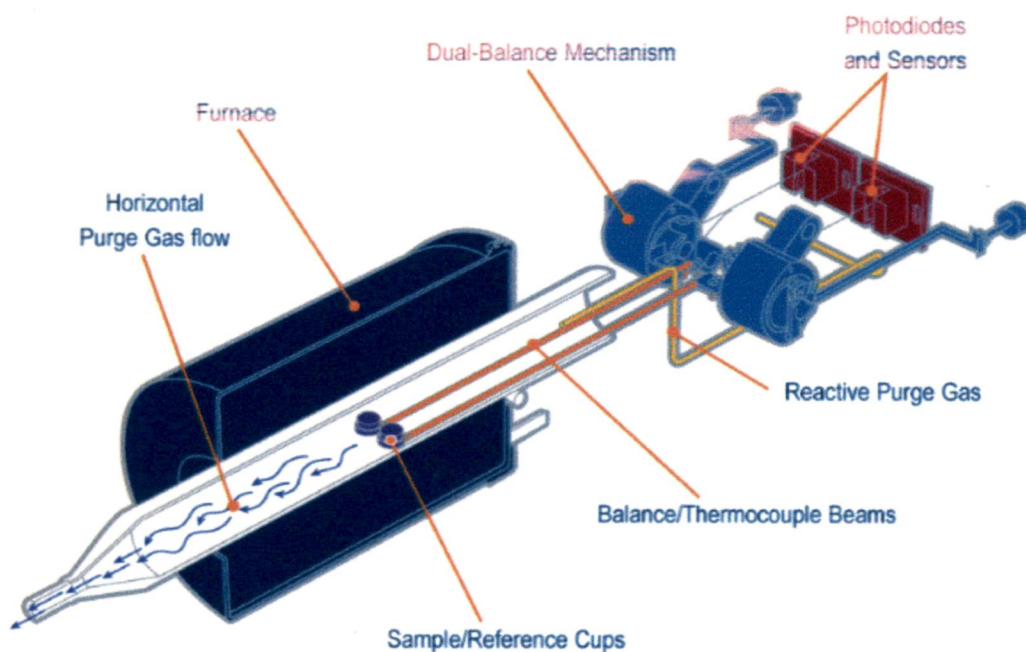

Fig. 4.10 DTA Apparatus (

The key features of a differential thermal analysis kit are as follows:
  ➢ Sample holder comprising thermocouples, sample containers and a ceramic or metallic block.

- Furnace.
- Temperature programmer.
- Recording system.

The essential requirements of the furnace are that it should provide a stable and sufficiently large hot zone and must be able to respond rapidly to commands from the temperature programmer. A temperature programmer is essential in order to obtain constant heating rates. The recording system must have a low inertia to faithfully reproduce variations in the experimental set up. The sample holder assembly consists of a thermocouple each for the sample and reference, surrounded by a block to ensure an even heat distribution. The sample is contained in a small crucible designed with an indentation on the base to ensure a snug fit over the thermocouple bead. The crucible may be made of materials such as Pyrex, silica, nickel or platinum, depending on the temperature and nature of the tests involved.

CHAPTER 5

EXPERIMENTAL DETAILS

Sol-gel synthesis of HAp

In the synthesis of the sol-gel HAp water was employed as the diluting media. Triethyl phosphite (HIMEDIA, Laboratory grade) sol was diluted in water. The molar ratio of water to the phosphorous precursor was kept at 3. The mixture was sealed in a glass beaker immediately after the addition of water, the it was stirred vigorously. Due to the immiscibility between the phosphite sol and water, the mixture initially appeared opaque, light being scattered by the emulsion phase. However, the emulsion transformed into a clear solution after approximately 30 minutes of mixing, suggesting that the phosphite was completely hydrolyzed. This was also confirmed by the loss of the characteristic phosphite odor of the mixture. A stoichiometric amount (i.e to maintain Ca/P = 1.67) of 3M Calcium nitrate tetrahydrate (Merck, UN 1454), dissolved in water, was subsequently added dropwise into the hydrolyzed phosphorous sol. Vigorous stirring was continued for an additional 10 minutes after addition. As a result of this process, a clear solution was obtained and aged at room temperature for 16 hrs before drying. The solvent was then driven off at 60°C until a viscous liquid was obtained. The corresponding HAp concentration changed from 3.6 vol% (in the solution) to 13.6 vol% (in viscous liquid), the calculation based on the final volume of HAp powder after calcinations. Further drying of the viscous liquid at 60°C resulted in a white gel. The gel was ground with a mortar and pestle into fine powder and subjected to different temperatures i.e. 400°C, 750°C and 1200°C for 2 hrs.

The HAp phase derived from the above sol-gel process was detected by an X-ray diffractometer (Brueker D8 Advance) with 2θ angle range of 20-60°, at 1°/min scanning rate using Cu Kα ($\lambda = 0.154\ 18$ nm) operated at 30 KV and 20 mA. The microstructure of the powder was examined using Field effect scanning

electron microscopy (FESEM, FEI Company). Elemental analysis of Ca and P was conducted using Energy dispersive X-ray spectroscopy (EDAX).
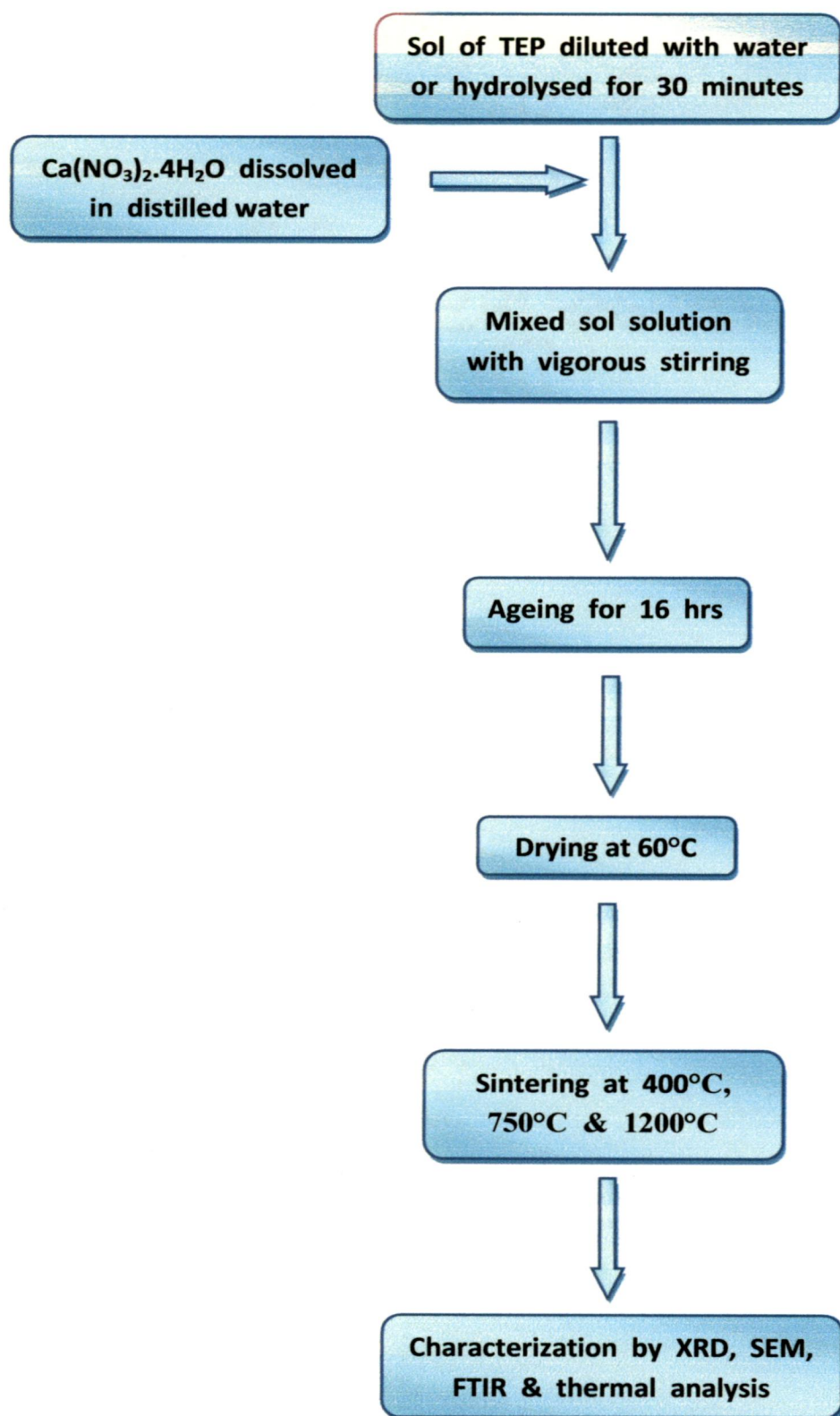

Fig. 5.1 Flow chart of aqueous sol-gel synthesis and characterization of Hydroxyapatite

The ground gel powder was also examined by Thermogravimetric analyser, (Perkin Elmer, Pyris Diamond) from room temperature to 1000°C at a rate of 10°C/min with Alumina as the reference in nitrogen environment, to monitor the weight loss of the organic residues. Fourier transform infrared spectrometer (FT-IR, Nicolet Nexus) in the range of 400-4000 cm^{-1} in absorption mode was used to examine the structure in those dried and sintered gels. For IR sample preparation, 2 mg of powder sample was thoroughly mixed with 200 mg of KBr using a mortar and pestle, followed by pressing at 100 MPa to form pellets. X-ray diffraction and FT-IR analyses were used for structural characterization.

CHAPTER 6

RESULTS AND DISCUSSION

6.1 Thermal Analysis

6.1.1: TGA

Result of the Thermogravimetric analysis of the HAp sample is shown in fig. 6.1 where three major weight loss stages can be easily distinguished. The characteristics temperature regions are 30-100°C, 100-400°C, and 400-550°C. In the first region, a sharp weight loss by 10.8% was observed, which indicates the evaporation of adsorbed water. The second region, showing 5.3% weight loss, reveals a slow removal of residuals, such as structural water and the organic residues, whereas the third stage shows the decomposition of nitrate compounds, leading to approximately 14% weight loss [35].
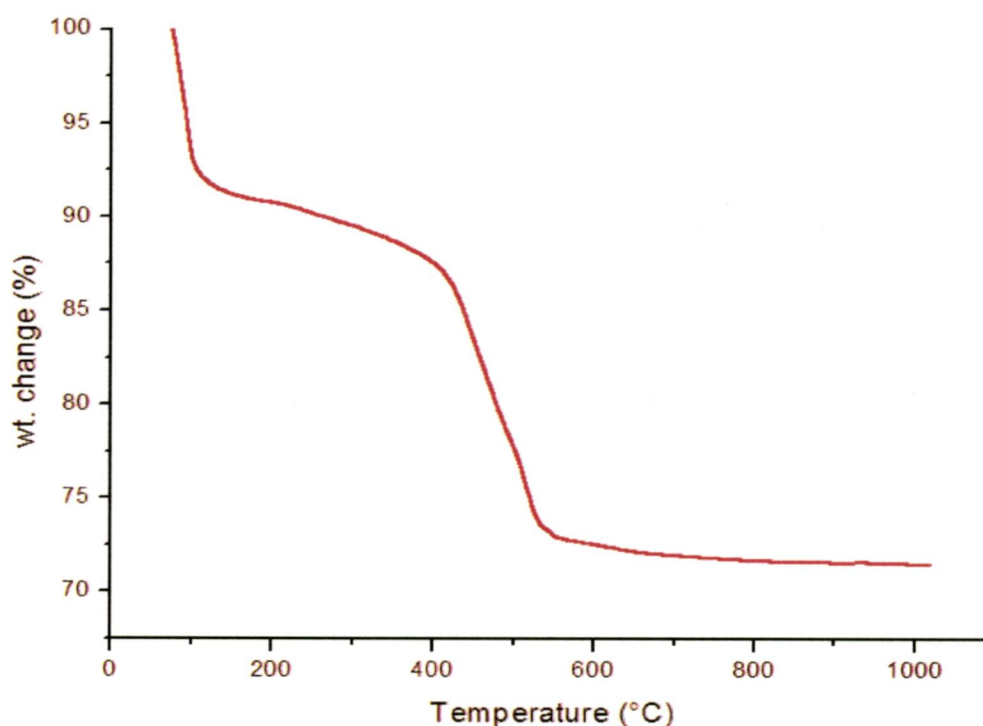

Fig. 6.1 TGA curve of HAp

Upon a close inspection a slight and gradual decrease in TGA curve was observed from 550°C to 820°C, corresponding to a weight loss of about 1.3%, suggesting a further removal of structural water due to decomposition and also the removal of CO_2. However, no further change in weight was detected upon further heating to 1000°C, indicating the decomposed phases are thermally stable. The HAp gel showed a total weight loss of about 30%. This corresponds to a 70 % yield of HAp gel.[1][35]

6.1.2: DTA

Differential thermal analysis shows an endothermic peak at about 100°C, which corresponds to evaporation of residual volatiles like water, followed by a small exothermic peak at about 400°C for HAp phase crystallization, and an endothermic peak at about 500°C as a result of HAp phase formation. . The differential thermal analysis is consistent with the weight loss curve and also confirmed by the phase identification in XRD.[3]
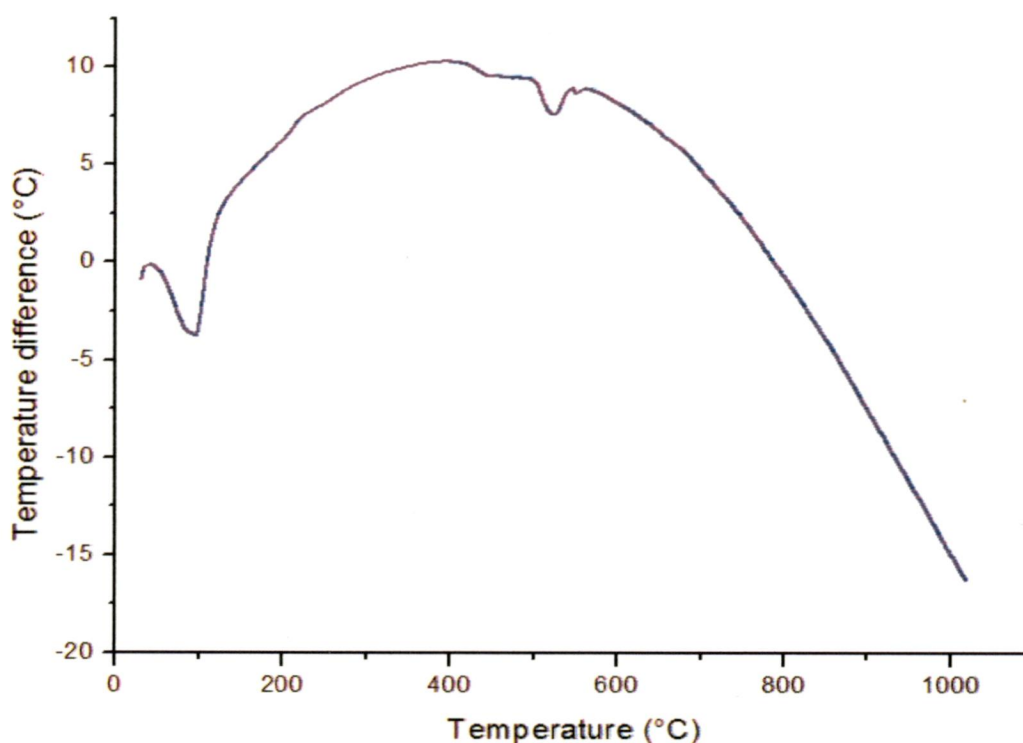

Fig .6.2 DTA curve of HAp

6.2: XRD Analysis

The XRD patterns of HAp gel without sintering and after sintering at 400°C, 750°C, and 1200°C are shown in fig 6.3. The d spacing of the sol–gel prepared powder are compared with the JCPDS card no. [09-432] standard for HAp. There is a good match with the standard both in terms of d-spacing and position of the peaks.
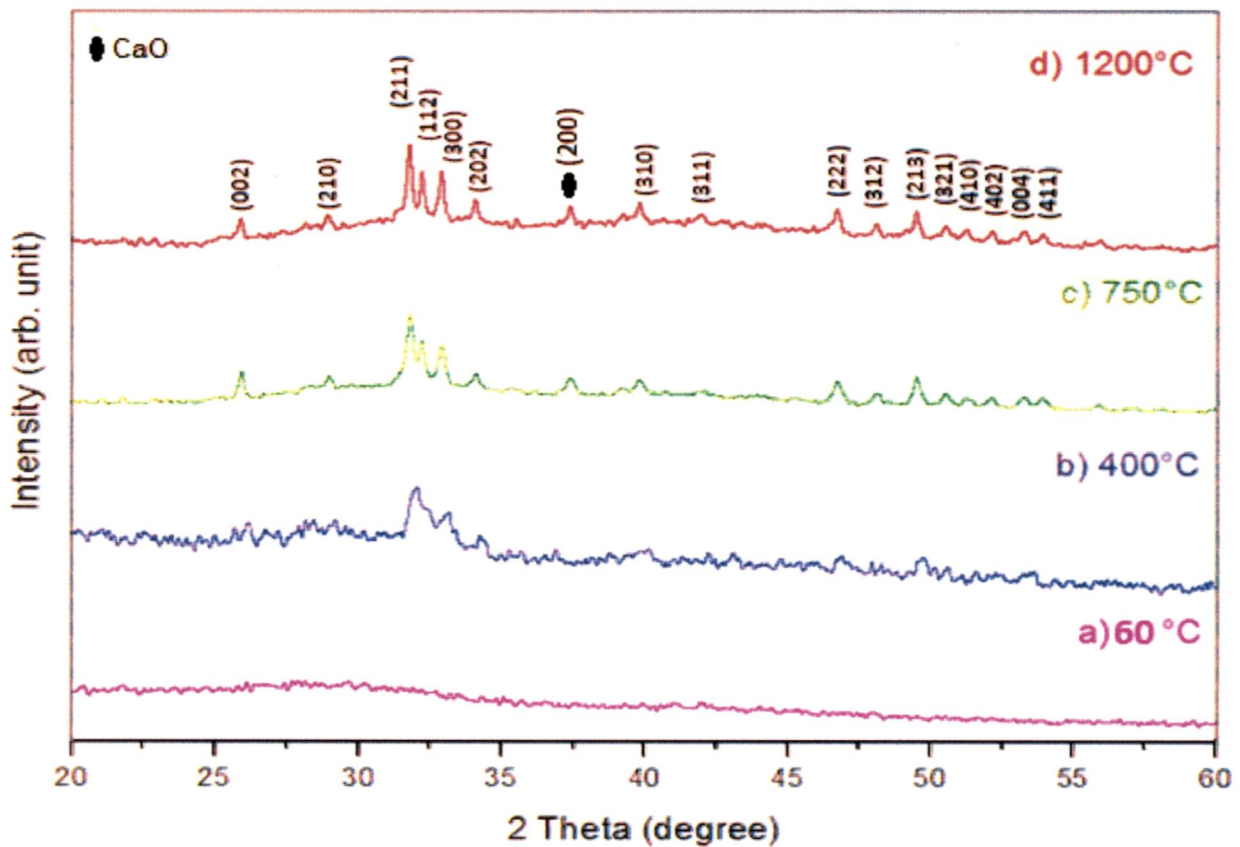

Fig. 6.3 XRD pattern HAp

Several major peaks, i.e. (002), (211), (112), (300), and (202), are seen, which are the characteristic peaks of the hydroxyapatite material, indicating the formation of the apatitic structure. Small amount of CaO was detected in the samples sintered at 750°C and 1200°C, suggesting the decomposition of HAp.[36]

40

No crystalline HAp phase could be observed in the dried gel based on the XRD pattern as is shown in Fig. 6.3 (a), indicating that HAp remained amorphous without sintering. The plane spacings of the sample are compared to the standard HAp (JCPDS #74-0566) in Table 2 [37]:

Table 2 : Plane spacings and intensities obtained from XRD

d (nm) spacing experimental	d (nm) spacing JCPDS	(hkl)
0.3437	0.3440	002
0.2812	0.2814	211
0.2777	0.2778	112
0.2720	0.2720	300
0.2628	0.2631	202
0.2297	0.2295	212
0.2263	0.2262	310
0.2147	0.2148	311
0.1943	0.1943	222
0.1890	0.1890	312
0.1840	0.1841	213
0.1806	0.1806	321
0.1782	0.1780	410
0.1754	0.1754	402
0.1719	0.1722	004

The effect of sintering temperature on the formation of HAp can be seen in Fig. 6.3. The sintering temperature plays an important role on the formation of HAp. As the sintering temperature is increased from 400 to 1200°C, several peaks of XRD pattern which belong to the HAp powder become more distinct and, also the widths of the peaks become more narrow, which suggests an increase in the degree of powder crystallinity [9]. It can also be seen that another crystalline

phase (CaO) appears at 750°C at $2\theta = 37.5°$. No other crystalline phase is present besides HAp at 400°C. It could be concluded that HAp could be decomposed into CaO as the sintering temperature increase to temperature at 750°C or above. The reaction is proposed as follows [37]:

$$Ca_{10}(PO_4)_6(OH)_2 \rightarrow 3Ca_3(PO_4)_2 + CaO + H_2O \qquad (6.2)$$

It has been reported that HAp decomposed within the temperature range of 600–800°C, and the decomposition temperature strongly depends on the characteristics and synthetic technique of the HAp powder.The width of the (002) peak at $2\theta = 25.9°$ of the apatitic structures sintered at different temperatures i.e. 400°C, 750°C and 1200°C was examined. The half-intensity width of the (002) peak decreased gradually, accompanied by improved sharpness of other major peaks, as the sintering temperature increased from 400°C to 1200°C. This observation indicated an increase in the crystallite size and/or improved crystal structure of the sintered HAp powder. However previous XRD analysis (fig.6.3) may suggest that the change in the half-intensity width of the (002) peak is attributed mainly to crystal growth. A decreased intensity of the half-intensity width for (002) crystal plane is then suggestive of improved crystallinity along the crystallographic c-axis at elevated temperature.

Table 3 : The lattice parameters calculated for the sintered samples

Sintering temperature (°C)	Lattice constant, a (Å)	Lattice constant, c (Å)	Cell volume, V (Å)^3
400	9.419	6.821	524.10
750	9.420	6.874	528.26
1200	9.416	6.886	532.76

It should be noted that the crystallization of the apatitic phase started to occur at about 400°C, a temperature which is lower by about 200°C compared to those in the literature. A greater amount of hydroxyl species (primarily from initial water addition) evolved in the gel phase may be responsible for low-temperature crystallization. Based on above observations, this water based sol-gel route seems to provide an attractive alternative for HAp synthesis, especially compared to the only alkoxide based processes [35].

6.3: FTIR Analysis

The FTIR spectra of the sintered and the dried gel are shown in the fig.6.4. The dried gel exhibits amorphous material bands. The as dried sample showed sharp peaks at 920 and 740 cm^{-1}, which correspond to the NO_3^- group. Also the presence of strong and broad bands at 3390 cm^{-1} denotes the unhydrogen bonded -OH stretching. Therefore, the IR spectrum for the as-dried powder sample represents the presence of calcium nitrate. There is a broad envelope between 3700 and 2700 cm^{-1} due to the O-H stretch of water and HAp. The O-H groups are hydrogen bonded The bands, in the HAp powder sintered at 400°C and 750°C, at 1463 cm^{-1}, 1414 cm^{-1} and a sharp band at 876 cm^{-1} correspond to the association of carbonate ion with the apatitic phase. The relative intensity of these bands shows that the carbonate content decreased with the increasing sintering temperature due to removal of CO_2 at higher temperature as indicated by TGA analysis also.

The first indication of the formation of Hydroxyapatite structure is in the form of band centered at about 1050 cm^{-1} in the HAp samples sintered at 400°C, 750°C, and 1200°C which is in agreement with the XRD analysis. The spectra of HAp heated to 750°C and 1200°C show the bands corresponding to Hydroxyapatite, carbonate ion and Calcium hydroxide (3641 cm^{-1}). The calcium oxide bands can not be detected as the bands corresponding to Ca-O stretching modes would lie in the near IR region at wavenumbers below 400 cm^{-1}[4]

[34][35] . The triply degenerate v_4 bending vibrations of PO_4^{3-} ions at 604 and 570 cm^{-1} indicate the formation of HAp phase in all the sintered samples.[40]
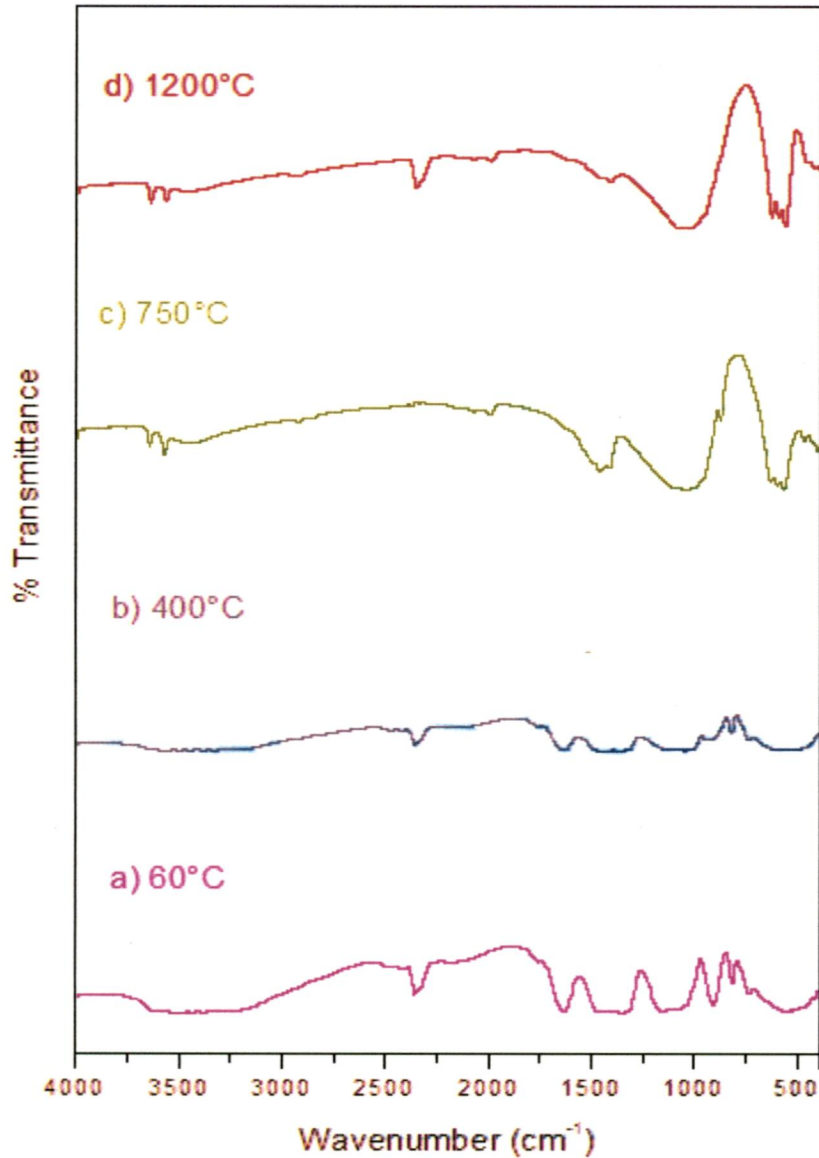

Fig. 6.4 FTIR spectra of HAp

Formation of Hydroxyapatite occured at a relatively low temperature of about 400°C, which was also shown by the XRD and Thermal analysis. Further heating at higher temperature resulted in the increase in the intensity of bands corresponding to Hydroxyapatite. Theoretically, there are four vibrational modes present for phosphate ion v_1, v_2, v_3 and v_4 all the four modes are IR active and are observed in HAp spectra. The v_1 and v_3 phosphate bands in the region of

44

900-1200 cm^{-1} and v$_4$ absorption bands in the region of 500-700 cm^{-1} are used to characterize apatite structure. The spectral bands in the range 900-1200 cm^{-1} containing symmetric v$_1$ and asymmetric v$_3$, P–O stretching modes of the phosphate groups were observed The band at about 960 cm^{-1} corresponds to v$_1$ symmetric P-O stretching vibration of the PO$_4^{3-}$ ion. The distinguishable presence of these bands together with the bands at about 604 cm^{-1} and 570 cm^{-1} corresponding to the triply degenerate v$_4$ bending vibration of the PO$_4^{3-}$ indicate the increased quality of Hydroxyapatite at these temperatures [35]. The bands 1420 and 1465 cm^{-1} of the heated samples at 750°C, and 1200°C show a decrease in intensity while the bands assigned to the stretching and absorption band of Hydroxyapatite (3570 and 636 cm^{-1}) are observed, which are characteristics of the stoichiometric Hydroxyapatite [12][4].

It should be noted that absorption bands at 3581, 3561, 3487, 3320, 2430, 1283 and 917 cm^{-1}, which distinguish the formation of octacalcium phosphate are absent and that confirms the HAp stoichiometry. The characteristic peaks for TCP reported at 950 and 975 cm^{-1} were also absent in the stoichiometric HAp.

Table 4 : Vibrational frequencies and the corresponding groups

Vibrational frequency (cm^{-1})	Assignment
3700 – 2700	hydrogen bound O-H stretch of HPO$_4^{2-}$ and water
1463	Carbonate ion vibrations
1414	Carbonate ion vibrations
1100	P-O asymmetric stretching
1050	P-O asymmetric stretching
920 and 740	Nitrate ion vibrations
960	v$_1$ symmetric P-O stretch of PO$_4^{3-}$
604	PO$_4^{3-}$ bending vibrations
570	PO$_4^{3-}$ bending vibrations

6.4: Microstructural Examination

6.4.1: Crystallite size

The crystallite size of the dried and sintered gel was calculated using the Scherrer equation:

$$\tau = \frac{K\lambda}{\beta \cos \theta} \qquad (6.3)$$

Where K is the shape factor and its value is about 0.9, λ is the wavelength of the X-ray used for diffraction i.e. 0.154 nm , β is the line broadening at half the maximum intensity (FWHM) in radians and θ is the Bragg angle. τ is the mean size of the ordered domain in nm, which may be smaller or equal to the grain size. The (002) peak was the most distinct reflection in the XRD pattern. Therefore, the line broadening of the (002) reflection was used to calculate the mean crystallite size by the Scherrer's formula. The crystallite size was calculated along the c-axis (long dimension) of the HAp crystals.
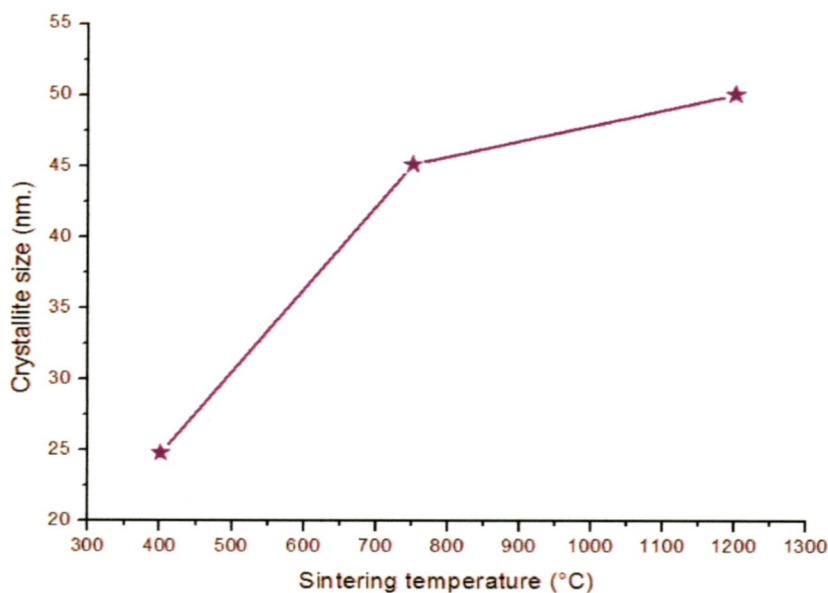

Fig. 6.5 Crystallite size vs. Sintering temperature of HAp

Figure 5.4 shows the resulting crystallite size calculated for the dried samples as a function of the sintering temperature. It is evident that crystal growth contributes to the increase in reflection intensity as depicted in fig. 5.3. the crystallite size obtained for the gel sintered at 400°C was 24.78 nm, and that calculated for the gel sintered at 750°C was 45.09 nm, and the crystallite size obtained for the gel sintered at 1200°C was 50.02 nm.

6.4.2: FESEM Analysis

The microstructures of Hydroxyapatite bioceramics were observed using scanning electron microscopy. Figures below illustrate the typical SEM photographs of Hydroxyapatite powder sintered at different tempuratures. The mean size of the grains was found to increase with the increasing sintering temperature which is in agreement with the crystallite size analysis, which was also found to be increasing with the increased sintering temperature.
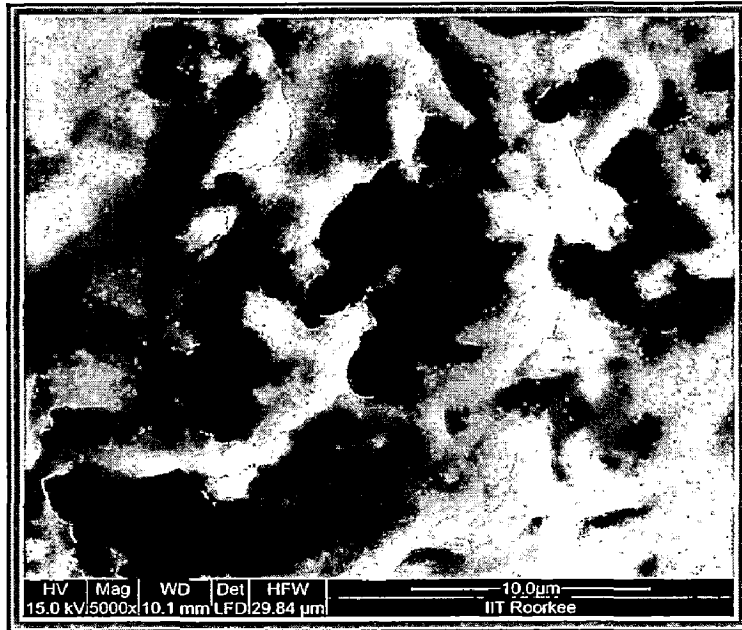

Fig. 6.6 HAp dried gel

Fig. 6.7 HAp powder sintered at 400°C
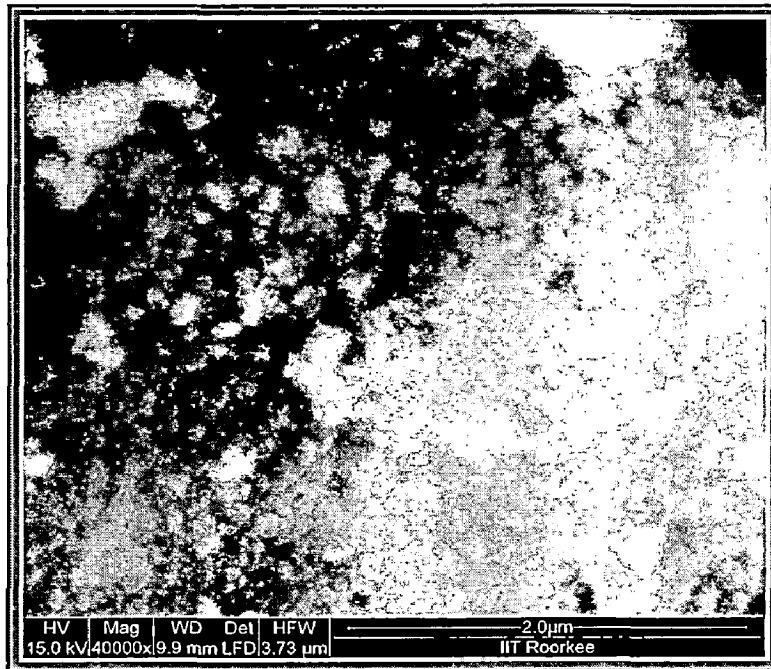

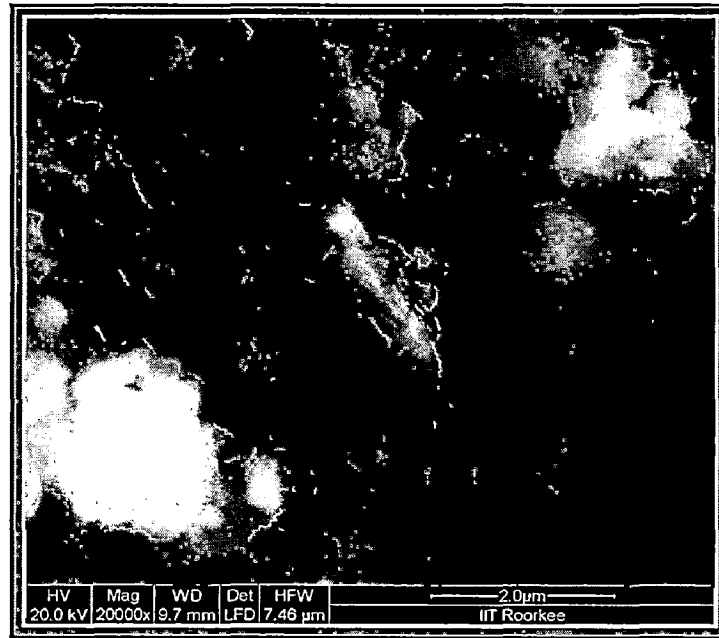*Fig. 6.8 HAp powder sintered at 750°C*

Fig. 6.9 HAp powder sintered at 1200°C

The HAp dried gel and the HAp powder sintered at 400°C did not show any distinguishable grain or any particular morphology. There are only agglomerates of different sizes seen in the micrograph of these two samples. Also, the HAp powder sintered at 400°C showed the occurance of pores between the agglomerated structures. The figures 5.8 and 5.9 show the morphologic characteristics of the particles of hydroxyapatite sintered at 1200°C, which indicates that the material is a homogeneous powder. There are many spherical agglomerations and crystallites of uniform size with pores between them were observed. The average grain size for the HAp sintered at 750°C was found to be about 250 nm which increased to be around 350 nm for the powder sintered at 1200°C. At higher temperature, the material agglomerate in bigger size due to the growth of crystalline phases and the pores were also seen. These pores are beneficial for the circulation of the physiological fluid throughout the coatings when it is used as biomaterials.

6.5 EDAX Analysis

The respective EDAX spectra show the obvious presence of all the constituent elements, viz., Ca, P, and O in the HAp powder samples.
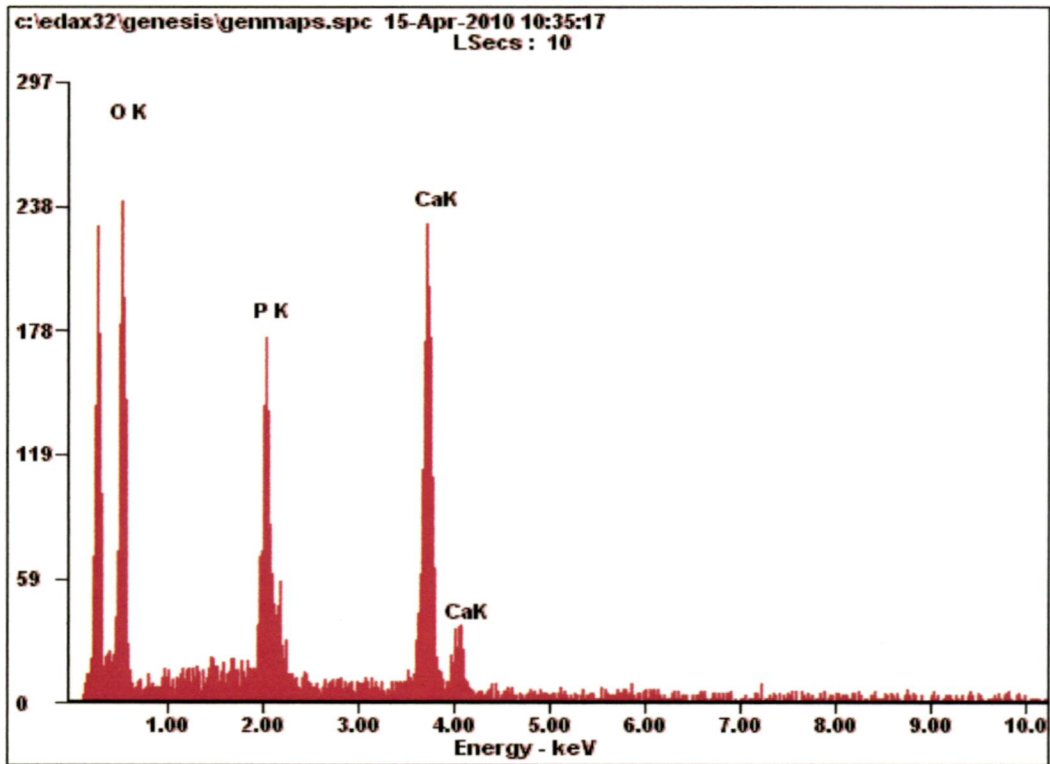

Fig. 6.10 EDAX spectrum of HAp sintered at 400°C

The Ca/P ratio of the HAp was analysed by the energy dispersive X-ray analysis. Theoretically the Ca/P ratio for the standard stoichiometric HAp ($Ca_{10}(PO_4)_6(OH)_2$, Ca/P=10/6) molecule should be 1.67.

The Ca/P ratio exhibited by the HAp powder sintered at 400°C was found to be 1.67 ± 0.3. the measurements were done at different areas of the HAp powder.

The EDAX analysis of the Hydroxyapatite powdes sintered at 750°C showed a Ca/P ratio near to the stoichiometrical ratio of the standard Hydroxyapatite powder. It showed the Ca/P ratio of 1.72 ± 0.3.
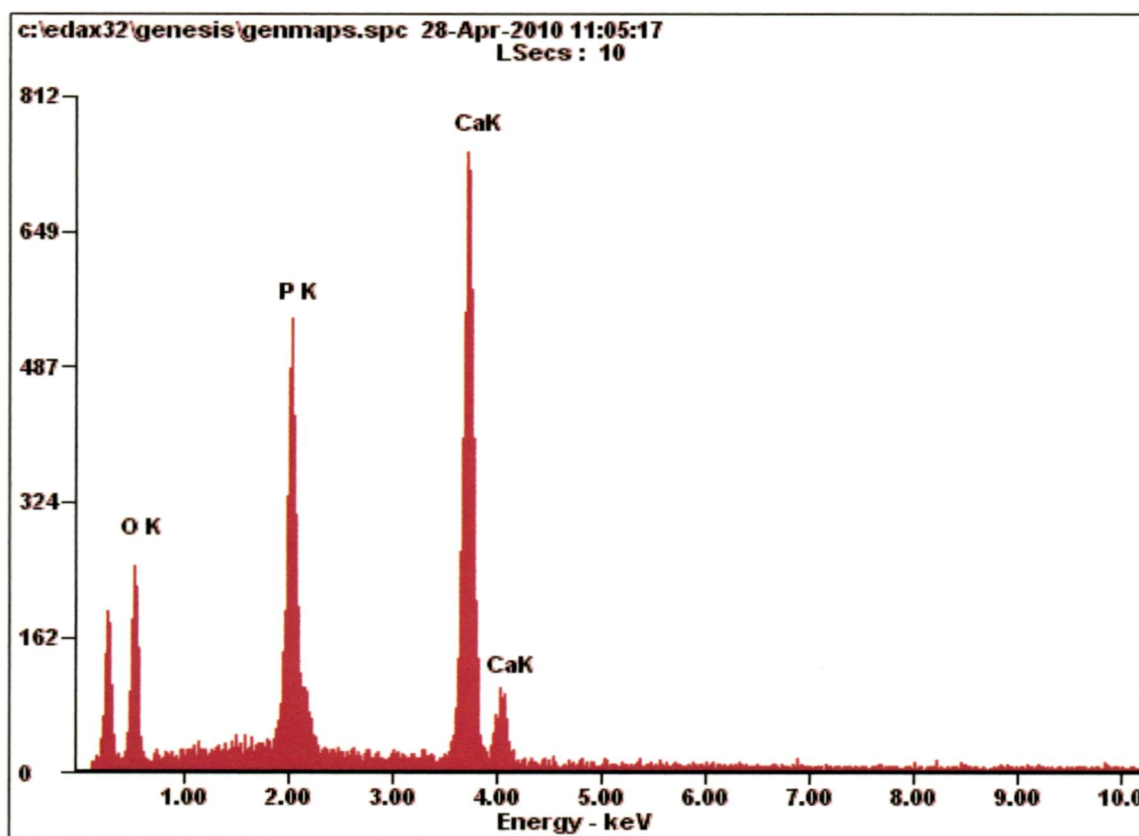

Fig. 6.11 EDAX spectrum of HAp sintered at 750°C

The EDAX pattern of Hydroxyapatite powder sintered at 1200°C showed the Ca/P ratio of 1.71 ± 0.3. The HAp powder sintered at 750°C showed some minor peaks of CaO in the XRD pattern. Studies by Chai and Ben-Nissan (1999) indicate that phosphorus containing precursors have high potential for volatilization

above 650°C (Szu et al 1992), hence $Ca(NO_3)_2$ molecules may not get completely incorporated into the complex which is evident by higher Ca/P molar ratio at 750°C and above [36].
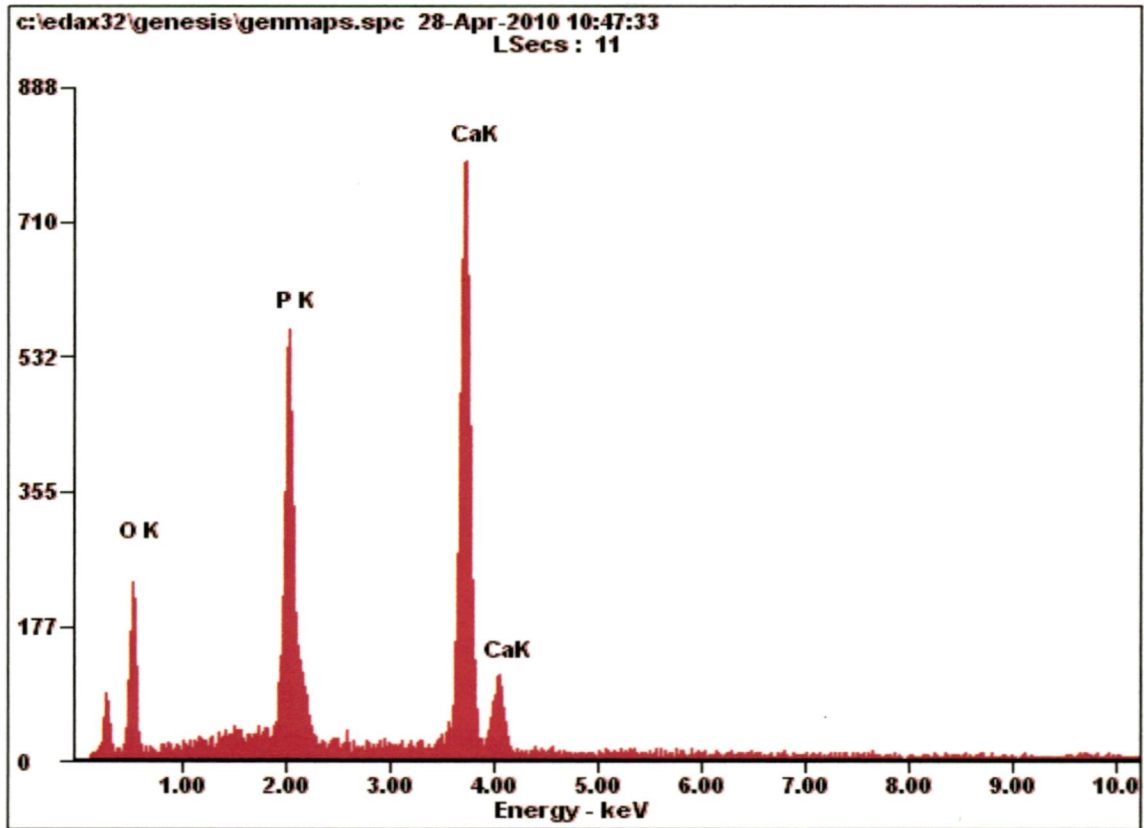

Fig. 6.12 EDAX spectrum of HAp sintered at 1200°C

The presence of the C-kα peak (at the extreme left) is due to the electron beam induced contamination, which was built-up during fine-probe electron beam irradiation while acquiring EDAX spectra.

CHAPTER 7

CONCLUSION

Water based sol-gel non-stoichimetric Hydroxyapatite was successfully synthesized and characterized using the alkoxide-salt precursor system including Triethyl phosphite and Calcium nitrate salt as phosphorous and calcium precursors respectively. The above process for HAp synthesis allows the phase formation in hydroxyapatite at a relatively low temperature, i.e. about 400°C, as compared to the other processes, including other precursors, in which the phase formation occurs at around 500°C. The ageing time was also less than the other sol-gel processes i.e. 16 hrs. The use of highly chemically active Triethyl phosphite (III), as compared to other less active precursors may be responsible for the enhanced reactivity in this triethyl phosphite/calcium nitrate route of HAp synthesis. The presence of large amount of hydroxyl species originating from the initial water content may also be responsible for the low temperature synthesis of HAp in this water based route. The sintered powder showed the presence of trace amount of CaO. The low temperature formation of the HAp powder was also confirmed by FT-IR and thermal analysis by DTA and TGA. The SEM micrograph showed the formation of uniform sized grain with porosity. The Ca/P ratio was determined using the EDAX spectra which was slightly more than the stoichiometric ratio.

REFERENCES

1. C. S. Chai and B. Ben-Nissan, "Bioactive nanocrystalline sol-gel hydroxyapatite Coatings", Journal of Materials Science- Materials in Medicine, 10, 465-469 (1999)

2. Hossein Eshtiagh-Hosseini, Mohammad Reza Housaindokht, Mohammad Chahkandi, "Effects of parameters of sol–gel process on the phase evolution of sol–gel-derived hydroxyapatite", Materials Chemistry and Physics, 106, 310–316 (2007)

3. Dean-Mo Liu, Quanzu Yang, Tom Troczynski, Wenjea J. Tseng, "Structural evolution of sol–gel-derived hydroxyapatite", Biomaterials, 23, 1679–1687 (2002)

4. A. Ruban Kumar and S. Kalainathan, "Growth and characterization of nano-crystalline hydroxyapatite at physiological conditions", Cryst. Res. Technol., 43, No. 6, 640 – 644 (2008)

5. Huipin Yuan, Zongjian Yang, Yubao Li, Xingdong Zhang, J. D. De Bruijn, K. De Groot, "Osteoinduction by calcium phosphate biomaterials", Journal of Materials Science: Materials in Medicine, 9, 723-726 (1998)

6. Larry L. Hench, "Bioceramics: From Concept to Clinic", J. American ceramic soc., 74, [7], 1487-510 (1991)

7. Xiaolong Zhu, Oliver Eibl, Christoph Berthold, Lutz Scheideler and Jurgen Geis-Gerstorfer, "Structural characterization of nanocrystalline hydroxyapatite and adhesion of pre-osteoblast cells", Nanotechnology, 17, 2711–2721 (2006)

8. E. Boanini, A. Bigi, "Biomimetic synthesis of carbonated hydroxyapatite thin films", Thin Solid Films, 497, 53 – 57 (2006)

9. U. Vijayalakshmi, K. Prabakaran, S. Rajeswari, "Preparation and characterization of sol–gel hydroxyapatite and its electrochemical evaluation for biomedical applications", Journal of Biomedical Materials Research Part A, 87(3), 739-49 (2008)

10. Donglu Shi, "Introduction to biomaterials", Tshinghua university press – 2006, P. 253.

11. A. Beganskienė, O. Dudko, R. Sirutkaitis, R. Giraitis, "Water Based Sol-Gel Synthesis of Hydroxyapatite", Materials Science (MEDŽIAGOTYRA), Vol. 9, No. 4, 1392–1320 (2003)

12. Irma Bogdanoviciene, Aldona Beganskiene, Kaia Tonsuaadu, Jochen Glaser, H. Jurgen Meyer, Aivaras Kareiva, "Calcium hydroxyapatite, $Ca_{10}(PO_4)_6(OH)_2$ ceramics prepared by aqueous sol–gel processing", Materials Research Bulletin, 41, 1754–1762 (2006)

13. Il-Seok Kim, Prashant N. Kumta, "Sol–gel synthesis and characterization of nanostructured hydroxyapatite powder", Materials Science and Engineering, B 111, 232–236 (2004)

14. K. Sakamato, S. Yamaguchi, A. Nakahira, K. Kijima., M. Okajaki, "Transformation of α-TCP to hydroxyapatite inorganic media", Bioceramics, vol.-10, edited by L.Sedel and C.Rey, pp. 241-244 in proceedings of the 10th International Symposium on Ceramics in Medicine, Paris, france, oct. 1997

15. M.T. Fulmer and P.W. brown, "Hydrolysis of dicalcium phosphate dehydrate to hydroxyapatite", Matter Med.,9,197-202 (1998)

16. D. B. Haddow, P.F. James and R. Van Noort, "Sol-Gel Derived Calcium Phosphate Coatings for Biomedical Applications", J.sol-gel sci. tech.,13,261-265 (1998)

17. A. P. Ameen, R. D. Short, R. Johns, G. Schwach, "The surface analysis of implant Materials, The surface composition of a titanium dental implant material", Clinical Oral Implantation res., 4, 144 (1993)

18. P.K. Stephenson, M.A.R. Freeman, P.A. Revell, J. Germain, M. Tuke, C.J. Pirie, "The effect of hydroxyapatite coating on ingrowth of bone into cavities in an Implant", The Journal of Arthoplasty, Volume 6, Issue 1, Pages 51-58 (1991)

19. Mansho Itokazu, Yang Wenyi, Takaaki Aoki, Akira Ohara, Naoki Kato, "Synthesis of antibiotic-loaded interporous hydroxyapatite blocks by vacuum method and in vitro drug release testing," Biomaterials, Volume 19, Issues 7-9, 817-819 (1998)

20. W. Paul, C. P. Sharma, "Development of porous spherical hydroxyapatite granules: application towards protein delivery", Journal of Materials Science: Materials in Medicine, 10, 383-388 (1999)

21. K. A. Gross, C. S. Chai, G. S. K. Kannangara, B. Ben-Nissan and L. Hanley, "Thin hydroxyapatite coatings via sol–gel synthesis", Journal of Materials Science:Materials in Medicine, 9, 839-843 (1998)

22. Cameron S. Chai, Karlis A. Gross, Besim Ben-Nissan, "Critical ageing of hydroxyapatite sol–gel solutions", Biomaterials, Volume 19, Issue 24, Pages 2291-2296 (1998)

23. A. Jillavenkatesa, R. A. Condrate SR, "Sol–gel processing of hydroxyapatite", Journal of Material Science, 33, 4111-4119 (1998)

24. T. Brendel, A. Engel, C. Rüssel, "Hydroxyapatite coatings by a polymeric route", Journal of Material Science, Volume 3, 175-179 (1992)

25. T. Anee Kuriakose, S. Narayana Kalkura, M. Palanichamy, D. Arivuoli, Karsten Dierks, G. Bocelli, C. Betzel, "Synthesis of stoichiometric nano crystalline hydroxyapatite by ethanol-based sol–gel technique at low temperature", Journal of Crystal Growth, 263, 517–523 (2004)

26. D. B. Haddow, P. F. James, R. Van Noort, "Characterization of sol-gel surfaces for biomedical applications", Journal of Materials Science: Materials in Medicine, Volume 7, 255-260 (1996)

27. Wenjian Weng, J. L Baptista, "Sol–gel derived porous hydroxyapatite coatings", Journal of Materials Science: Materials in Medicine, Volume 9, 159-163 (1998)

28. F. H. Westheimer, Shaw Huang, Frank Covitz, "Rates and mechanisms of hydrolysis of esters of phosphorous acid", J. Am. Chem. Soc., 110 (1), 181–185 (1988)

29. Young R. A, Holcomb D. W., "Variability of hydroxyapatite preparations", Calcif Tissue Int.;34 Suppl 2:S17-32 (1982)

30. A. J. Ruys, M. Wei, C. C. Sorrell, M. R. Dickson, A. Brandwood, B. K. Milthorpe, "Sintering effects on the strength of hydroxyapatite", Biomaterials, Volume 16, Issue 5, 409-415 (1995)

31. L. D. Piveteau, M. I. Girona, L. Schlapbach, P. Barboux, J. P. Boilot, B. Gasser, "Thin films of calcium phosphate and titanium dioxide by a sol-gel route: a new method for coating medical implants", Journal of Materials Science: Materials in Medicine, 10, 161-167 (1999)

32. Y. Masuda, K. Matubara, S. Sakka, "Synthesis of Hydroxyapatite From Metal

Alkoxides Through Sol--Gel Technique", Journal of the Ceramic Society of Japan, Vol. 98, no. 11, 1255-1266 (1990)

33. Wenjian Weng, Liping Huang, Gaorong Han, "The alkoxide sol-gel process in the calcium phosphate system and its applications", Applied Organometallic Chemistry, Volume 13, Issue 8, 555 – 564 (1999)

34. Dean-Mo Liu, T. Troczynski, Wenjea J. Tseng, "Aging effect on the phase evolution of water-based sol–gel hydroxyapatite", Biomaterials ,23, 1227–1236 (2002)

35. Dean-mo liu, T. Troczynski, Wenjea J. Tseng, "Water based sol-gel synthesis of Hydroxyapatite: Process development", Biomaterials, 22, 11721-1730 (2001)

36. K. P. Sanosh, Min-Cheol Chu, A. Balakrishnan, T. N. Kim and Seong-Jai Cho, "Preparation and characterization of nano-hydroxyapatite powder using sol–gel Technique", Bull. Mater. Sci., Vol. 32, No. 5, 465–470 (2009)

37. M.H. Fathi, A. Hanifi, "Evaluation and characterization of nanostructure hydroxyapatite powder prepared by simple sol–gel method", Materials Letters, 61, 3978–3983 (2007)

38. Anbalagan Balamurugan, Jean Michel, Joel Faure, Hicham Benhayoune, Laurence Wortham, Ganesh Sockalingum, Vincent Banchet, Sylvie Bouthors, Dominique Laurent-Maquin, Gerard Balossier, "Synthesis and Structural Analysis of Sol Gel Derived Stoichiometric Monophasic Hydroxyapatite", Ceramics – Silikáty, 50, (1), 27-31 (2006)

39. Qiuhua Yuan, Laxmi Kumari Sahu, Nandika A. D'Souza, Teresa Diane Golden, "Synthesis of hydroxyapatite coatings on metal substrates using a spincasting Technique", Materials Chemistry and Physics 116, 523–526 (2009)

40. Martin A. Encinas-Romero, Salvador Aguayo-Salinas, Santos J. Castillo, Felipe F. Castillon-Barraza, Victor M. Castano, "Synthesis and Characterization of Hydroxyapatite– Wollastonite Composite Powders by Sol–Gel Processing", Int. J. Appl. Ceram. Technol., 5 [4] 401–411 (2008)